Electronic Supplementary Material (ESI) for ChemComm.
This journal is © The Royal Society of Chemistry 2017

Electronic Supplementary Information (ESI)

Synthesis and Activation Potential of an Open Shell Diphosphine

Kai Helmdach, Stephan Ludwig, Alexander Villinger, Dirk Hollmann, Jutta Kösters and Wolfram W. Seidel

Institut für Chemie, Universität Rostock,
Albert-Einstein-Straße 3a, 18059 Rostock, Germany

Content:

1 Crystallographic details

1.1 Overview

Single crystals suitable for X-ray diffraction analysis were selected in Fomblin YR-1800 perfluoropolyether oil (Alfa Aesar) at ambient temperature and mounted on a glass fiber. During the measurement the samples were cooled to 100(2), 123(2) or 173(2) K. Diffraction data were collected on a Bruker-Nonius Apex X8 and a Bruker Kappa Apex II diffractometer using graphite monochromated Mo-K_α radiation. Structure solutions were found by direct methods (SHELXS-97 or SHELXS-2013)[S1] and were refined by full-matrix least-squares procedures on F^2 (SHELXL-2013)[S2]. All non-hydrogen atoms were anisotropically refined unless stated otherwise. Hydrogen atoms were included at calculated positions with fixed thermal parameters unless stated otherwise.

Table S1. Crystallographic details for **1b**, **2a**, **2b**, **3a** and **3b**.

	1b	**2a**	**2b**	**3a**	**3b**
empirical formula	$C_{22}H_{30}BN_7OW\cdot$ 1.23 CH_2Cl_2	$C_{33}H_{39}BIN_6OPW\cdot$ C_5H_{12}	$C_{34}H_{39}BN_7OPW\cdot$ 3.33 C_5H_{12}	$C_{45}H_{48}BIN_6OP_2W\cdot$ C_5H_{12}	$C_{46}H_{48}BN_7OP_2W\cdot$ 0.31 CH_2Cl_2
M_W / g·mol^{-1}	688.11	960.38	1025.43	1144.54	997.63
colour, habit	blue, needle	green, block	blue, block	blue, block	green, block
crystal system	monoclinic	orthorhombic	orthorhombic	monoclinic	monoclinic
space group	$P2_1/c$	$Pca2_1$	$Pca2_1$	$P2_1/n$	$P2_1/n$
a / Å	11.8346(4)	16.9669(5)	16.4962(10)	13.1010(5)	13.020(3)
b / Å	24.9365(8)	10.4622(3)	10.3883(7)	19.6181(8)	19.697(4)
c / Å	9.9552(3)	22.0079(7)	22.0051(16)	19.5916(8)	19.523(4)
α / °	90	90	90	90	90
β / °	114.209(2)	90	90	99.121(1)	96.911(9)
γ / °	90	90	90	90	90
V / Å^3	2679.54(15)	3906.6(2)	3771.0(4)	4971.7(3)	4970.1(18)
Z	4	4	4	4	4
$\rho_{calcd.}$ / g·cm^{-1}	1.706	1.633	1.806	1.529	1.333
μ / mm^{-1}	4.541	3.826	3.163	3.051	2.461
$\lambda_{MoK\alpha}$ / Å	0.71073	0.71073	0.71073	0.71073	0.71073
T / K	123	173	123	100	123
collected refl.	35866	57393	58646	77570	185332
unique refl.	7117	11563	11348	14625	13194
refl. $I > 2\sigma(I)$	5147	9396	7667	13043	11325
R_{int}	0.074	0.096	0.096	0.035	0.105
parameters/restraints	353/156	426/8	416/1	611/69	623/678
R_1 [$I > 2\sigma$(I)]	0.0398	0.0370	0.0491	0.0240	0.069
wR_2 (all data)	0.0761	0.0677	0.1067	0.0554	0.115
GooF	0.986	0.976	0.941	1.048	1.228
resid. density [eÅ^{-3}]	0.774/-0.990	1.315/–1.425	3.418/–1.590	1.202/–0.577	3.380/-4.860
CCDC	1502928	1502929	1502931	1502930	1502932

Table S2. Crystallographic details for **3a**-PF_6, **4a**-BF_4 and $[(Ph_2PC_2H_4PPh_2)N][BF_4]$.

	3a-PF_6	**4a**-BF_4	$[(Ph_2PC_2H_4PPh_2)N][BF_4]$
empirical formula	$C_{45}H_{48}BF_6IN_6OP_3W\cdot$ 0.6 CH_2Cl_2	$C_{45}H_{50}B_{1.96}F_{3.84}I_{1.04}N_7O_2P_2W\cdot$ 0.5 $C_4H_{10}O$	$C_{26}H_{24}BF_4NP_2$
M_W / g·mol^{-1}	1268.15	1229.84	499.21
colour, habit	brown, plate	orange, plate	colourless, needle
crystal system	monoclinic	triclinic	orthorhombic
space group	$P2_1/c$	P-1	$Pna2_1$
a / Å	13.1608(4)	12.6321(3)	17.0029(15)
b / Å	19.5011(6)	15.0895(3)	13.0353(13)
c / Å	20.3015(5)	26.9998(5)	10.6338(8)
α / °	90	78.394(1)	90
β / °	106.144(1)	84.668(1)	90
γ / °	90	80.515(1)	90
V / Å^3	5004.9(3)	4962.8(1)	2356.9(4)
Z	4	4	4
$\rho_{calcd.}$ / g·cm^{-1}	1.683	1.646	1.407
μ / mm^{-1}	3.148	3.100	0.232
$\lambda_{MoK\alpha}$ / Å	0.71073	0.71073	0.71073
T / K	123	123	123
collected refl.	161638	120390	19858
unique refl.	13268	27474	5164
refl. $I > 2\sigma(I)$	10606	16038	3695
R_{int}	0.0837	0.0733	0.1113
parameters/restraints	649/24	1276/64	338/20
R_1 [$I > 2\sigma$(I)]	0.0458	0.0540	0.0513
wR_2 (all data)	0.1006	0.0893	0.1377
GooF	1.259	1.007	0.814
resid. density [eÅ^{-3}]	2.316/–1.429	1.566/–2.758	0.296/–0.369
CCDC	1538644	1502933	1538645

1.2 Molecular structures of 1b, 2a/b, 3a/b, 3a-PF_6, 4a-BF_4 and [($Ph_2PC_2H_4PPh_2$)N][BF_4]

I. Molecular Structure of 1b

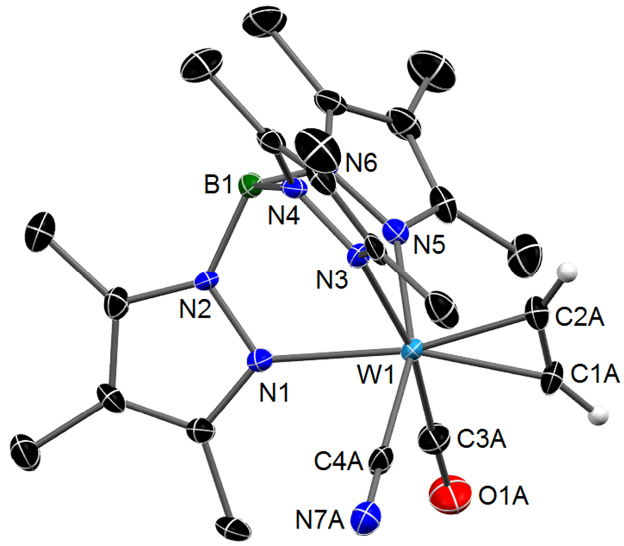

Figure S1. Molecular structure of **1b** in the crystal. Only one of the two disordered C_2H_2, CN, CO ligands sets is displayed. The second layer involves a CN/CO swap causing the alkyne to rotate about 90 ° to be aligned with the CO ligand again. Thermal ellipsoids are drawn at 50% probability. Hydrogen atoms (except for the acetylene hydrogen atoms) have been omitted for clarity. Selected bond lengths [Å] and angles [°]: W1–C1A 2.045(7), W1–C2A 2.014(7), W1–C3A 1.927(9), W1–C4A 2.156(9), W1–N1 2.234(3), W1–N3 2.201(4), W1–N5 2.215(4), C1A–C2A 1.276(9), C4A–W1–C3A 90.8(4).

II. Molecular Structure of 2a

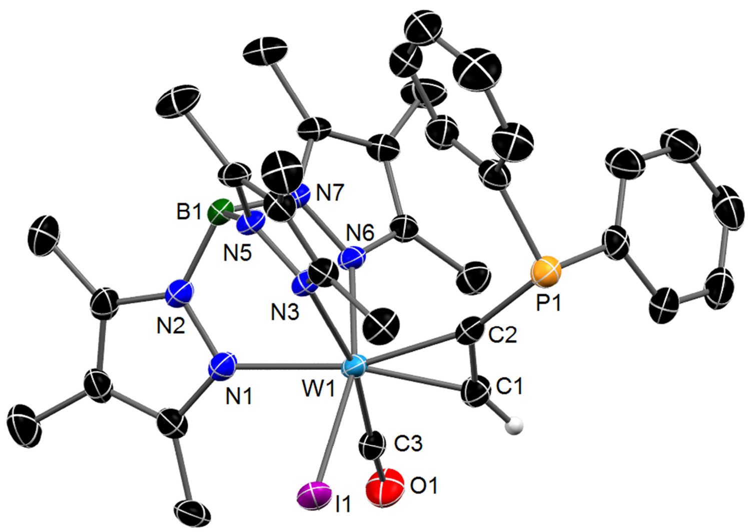

Figure S2. Molecular structure of **2a** in the crystal of **2a**·C_5H_{12}. Thermal ellipsoids are drawn at 50% probability. Co-crystallized pentane and hydrogen atoms (except for the alkyne hydrogen atom) have been omitted for clarity. Selected bond lengths [Å] and angles [°]: W1–C1 2.011(7), W1–C2 2.051(6), W1–C3 1.964(6), W1–I1 2.7897(5), W1–N1 2.220(5), W1–N3 2.242(4), W1–N6 2.182(5), C1–C2 1.311(9), C2–P1 1.787(6), C1–C2–P1 133.1(5).

III. Molecular Structure of 2b

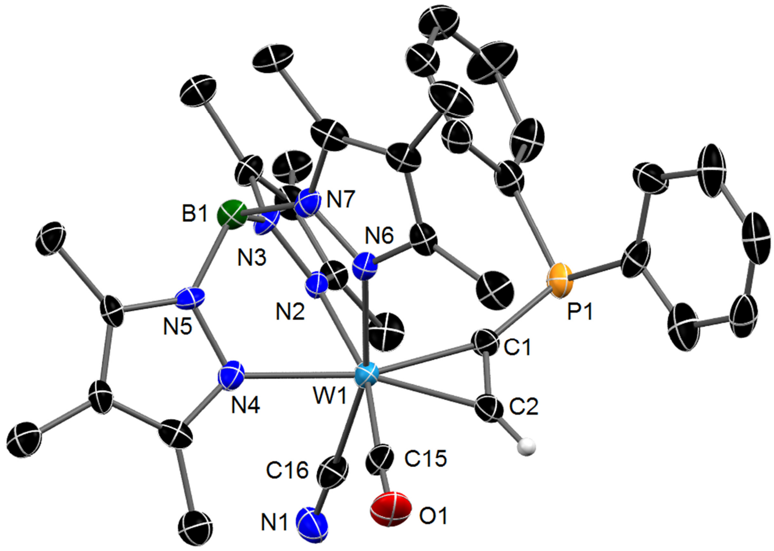

Figure S3. Molecular structure of **2b** in the crystal of **2b**·3.33 C_5H_{12}. Thermal ellipsoids are drawn at 50% probability. Co-crystallized pentane and hydrogen atoms (except for the alkyne hydrogen atom) have been omitted for clarity. Selected bond lengths [Å] and angles [°]: W1–C1 2.057(9), W1–C2 2.020(10), W1–C15 1.973(9), W1–C16 2.150(10), W1–N2 2.235(7), W1–N4 2.206(7), W1–N6 2.207(7), C1–C2 1.335 (13), C1–P1 1.779(9), C1–C2–P1 135.7(8).

IV. Molecular Structure of 3a

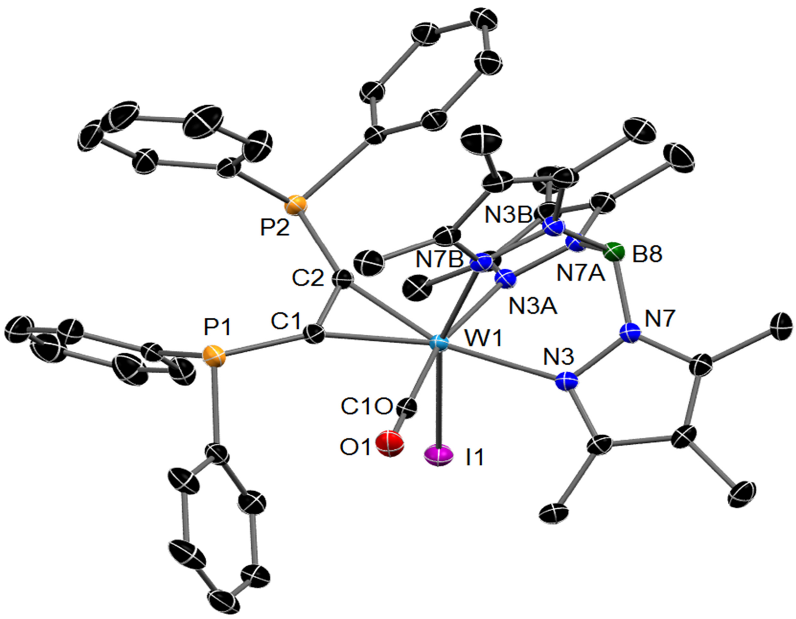

Figure S4. Molecular structure of complex **3a** in the crystal of **3a**·C_5H_{12} with thermal ellipsoids set at 50 % probability. Co-solvents, anions and hydrogen atoms have been omitted for clarity. Selected bond lengths [Å] and angles [°]: W1–C1 2.058(2), W1–C2 2.036(2), W1–C1O 1.966(2), W1–I1 2.7893(6), W1–N3 2.245(2), W1–N3A 2.234(2), W1–N7B 2.171(2), C1–C2 1.335(3), C1–P1 1.802(2), C2–P2 1.790(2), P1–C1–C2 133.7(2), C1–C2–P2 134.0(2).

V. Molecular Structure of 3b

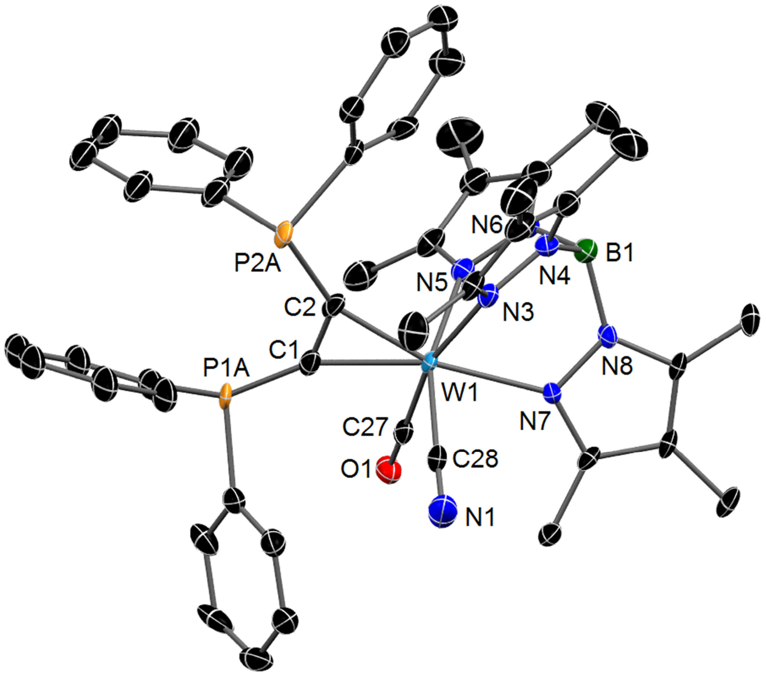

Figure S5. Molecular structure of **3b** in the crystal of **3b**·0.31 CH_2Cl_2. Only one of the slightly disordered alkyne positions is shown. Thermal ellipsoids are drawn at 50% probability. Co-crystallized CH_2Cl_2 and hydrogen atoms have been omitted for clarity. Selected bond lengths [Å] and angles [°]: W1–C1 2.071(5), W1–C2 2.032(5), W1–C27 1.973(6), W1–C28 2.138(6), W1–N3 2.226(5), W1–N5 2.196(5), W1–N7 2.224(4), C1–C2 1.332(8), C1–P1A 1.75(2), C2–P2A 1.82(4), P1A–C1–C2 139.7(9), C1–C2–P2A 133.8(12).

VI. Molecular Structure of 3a-PF_6

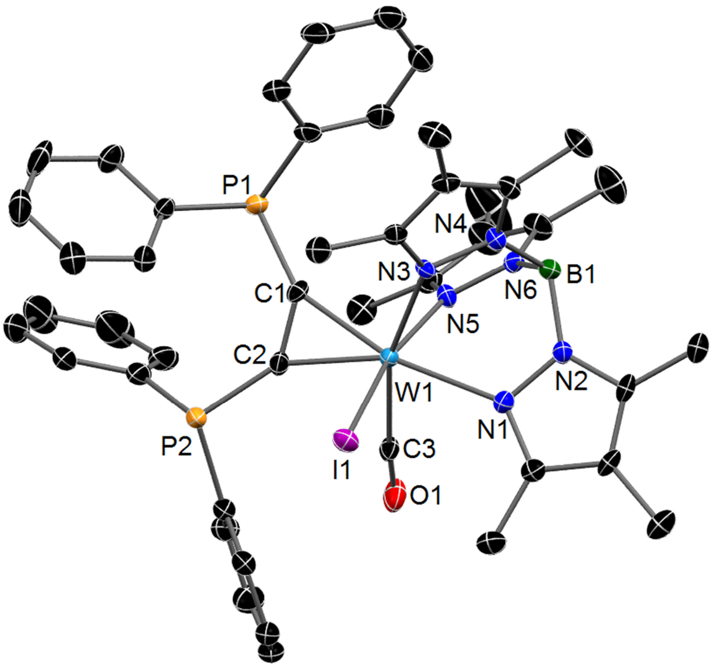

Figure S6. Molecular structure of cation **3a**$^+$ in the crystal of **3a**-PF_6·0.6 CH_2Cl_2 with thermal ellipsoids set at 50 % probability. Co-solvent, anion and hydrogen atoms have been omitted for clarity. Selected bond lengths [Å] and angles [°]: W1–C1 2.055(5), W1–C2 2.062(5), W1–C3 2.090(5), W1–I1 2.7276(4), W1–N1 2.234(4), W1–N3 2.178(4), W1–N5 2.138(4), C1–C2 1.345(7), C1–P1 1.766(5), C2–P2 1.779(5), P1–C1–C2 134.7(4), C1–C2–P2 137.1(4).

VII. Molecular Structure of 4a-BF_4

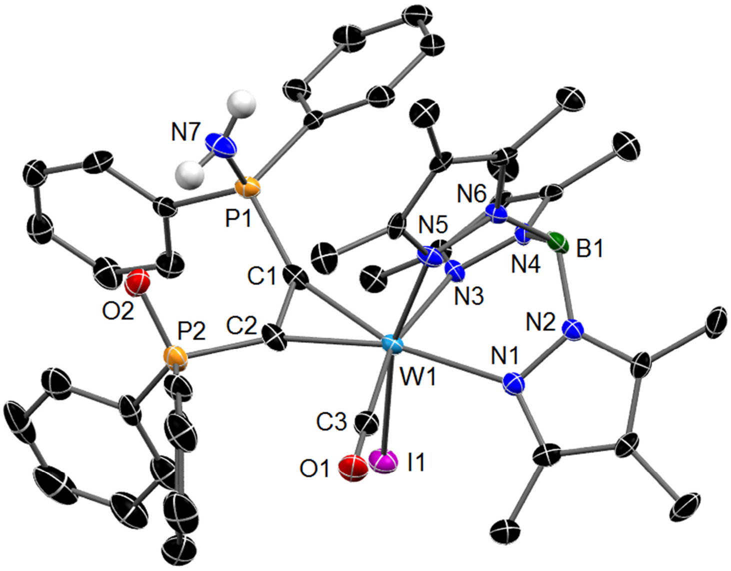

Figure S7. Molecular structure one of two independent cations **4a**$^+$ in the crystal of **4a**-BF_4·0.5 $C_4H_{10}O$ with thermal ellipsoids set at 50 % probability. Co-solvents, anions and hydrogen atoms (except for the amine hydrogen atoms in **4a**$^+$) have been omitted for clarity. Selected bond lengths [Å] and angles [°]: W1–C1 2.036(5), W1–C2 2.047(5), W1–C3 1.985(5), W1–I1 2.7740(7), W1–N1 2.209(4), W1–N3 2.187(4), W1–N5 2.248(5), C1–C2 1.323(7), C1–P1 1.770(5), C2–P2 1.825(5), P1–N7 1.609(5), P2–O2 1.486(4), P1–C1–C2 131.0(4), C1–C2–P2 127.2(4).

VIII. Molecular Structure of [($Ph_2PC_2H_4PPh_2$)N][BF_4]

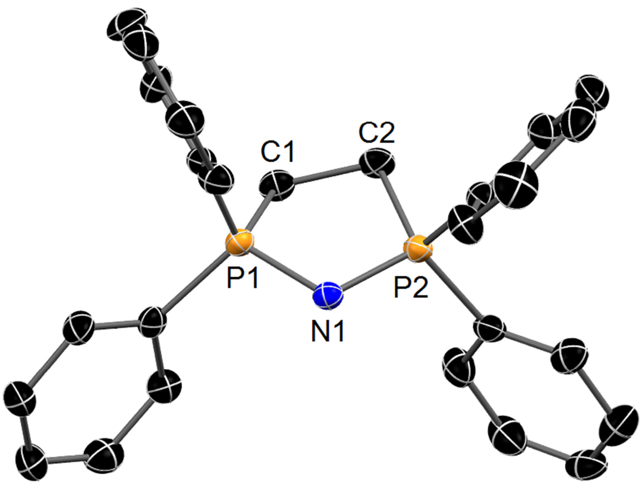

Figure S8. Molecular structure [($Ph_2PC_2H_4PPh_2$)N]$^+$ in the crystal of [($Ph_2PC_2H_4PPh_2$)N]**[**BF_4] with thermal ellipsoids set at 50 % probability. The anion and hydrogen atoms have been omitted for clarity. Selected bond lengths [Å] and angles [°]: N1–P1 1.611(4), N1–P2 1.610(4), C1–P1 1.820(5), C2–P2 1.840(5), C1–C2 1.553(8), P1–N1–P2 111.3(2), P1–C1–C2 104.4(3), C1–C2–P2 106.3(4).

2 Experimental section

2.1 General information

All operations were carried out in an atmosphere of dry argon using Schlenk and glove box techniques. Solvents were dried and saturated with argon by standard methods and freshly distilled prior to use. One- and two-dimensional NMR spectra were recorded at 300 K using Bruker Avance 250, 300 or 500 MHz spectrometer, respectively. In ^{1}H and ^{13}C NMR, the chemical shifts were internally referenced to the solvent residual peak. The ^{31}P NMR chemical shifts are referred to H_3PO_4 (85%) respectively. The $^{1}H/^{15}N$-HMBC spectra were obtained on a Bruker AVANCE 500 spectrometer and were referenced externally (33% (vol.) $MeNO_2$ in the corresponding solvent, $\delta_{reference}$ = 0 ppm). Chemical shifts $\delta(^{15}N)$ were calibrated internally by means of the "unified scale"[S5] with $\Xi(^{15}N)$ = 10.136767 MHz which corresponds to nitromethane at 0 ppm[S6]. They were determined by inverse-detected 2D NMR measurements (standard HMBC sequence, four pulses, gradient selection, transfer delay set to 100 ms corresponding to J(N,H) = 5 Hz; this works satisfactorily despite the fact that the coupling constants are actually smaller). IR spectroscopy was conducted on a Nicolet 380 FT-IR with a Smart Orbit ATR module. Elemental analyses were performed with a Thermo Finnigan Flash EA 1112 Series. Mass spectrometry was obtained with an Agilent 6210 Time-of-Flight LC/MS for electrospray ionization (ESI) and with a Thermo Electron Finnigan MAT 95-XP GC/MS for electron ionization (EI). UV/vis data was collected on a Perkin Elmer Lambda 19 spectrometer. EPR spectra were recorded on a Bruker ElexSys E 500 spectrometer. The starting materials KTp*[S7] (Tp* = hydridotris(3,4,5-trimethyl-pyrazolyl)borat), $[(C_5H_5)_2Fe][PF_6]$[S8] and $[(C_5H_5)Fe\{C_5H_4C(O)CH_3\}][BF_4$ or $PF_6]$[S8] were synthesized according to literature procedures. Technical acetylene was purified by passing successively a KOH and a P_2O_5 column prior to use. Commercial $[NO][BF_4]$ was purified by sublimation under reduced pressure before use. All other reagents were used as purchased from commercial sources.

2.2 Synthetic procedures

I. [NEt$_4$][Tp*W(CO)$_3$]

A suspension of W(CO)$_6$ (8 g, 22.7 mmol) and KTp* (8.59 g, 22.7 mmol) in 55 mL *N*,*N*-dimethylformamide was heated to 130 °C for 150 min in a Schlenk flask equipped with a condenser. During this time sublimed crystals of W(CO)$_6$ were removed into the solution by carefully shaking the flask. The resulting deep red solution was allowed to cool down to 60°C and was then poured into 130 mL of an aqueous solution of [NEt$_4$]Br (13 g, 62.0 mmol). The yellow precipitate was filtered, washed with water and diethyl ether, and dried *in vacuo*. Yield: 16.20 g (22.0 mmol, 97 %). **Elemental analysis** $C_{29}H_{48}BN_7O_3W$ (737.39 g mol^{-1}): C 47.01 (calcd. 47.24), H 6.24 (6.56), N 13.17 (13.40) %. **^{1}H NMR** (DMSO-d6, 300 MHz, 300 K): δ = 3.16 (q, ^3J = 7.18 Hz, 8 H, NCH_2CH$_3$), 2.34 (s, 9 H, CCH_3), 2.19 (s, 9 H, CCH_3), 1.80 (s, 9 H, CCH_3), 1.14 (t, ^3J = 7.18 Hz, 12 H, NCH$_2$CH_3) ppm. **^{13}C NMR** (DMSO-d6, 75 MHz, 300 K): δ = 225.3 (W*C*O), 148.6, 139.2, 110.2 (*C*CH$_3$), 51.5 (N*C*H$_2$CH$_3$), 13.8, 10.5, 8.1, (C*C*H$_3$), 7.1 (NCH$_2$*C*H$_3$) ppm. **IR** (ATR, cm^{-1}): $\tilde{\nu}$ = 2532 (w, BH), 1869 (s, CO), 1728 (s, CO).

II. Tp*W(CO)$_3$

To a stirred suspension of finely ground [NEt$_4$][Tp*W(CO)$_3$] (10 g, 13.56 mmol) in 100 mL acetonitrile was added [(C$_5$H$_5$)$_2$Fe][PF$_6$] (4.49 g, 13.56 mmol) in three portions. After 120 min the suspension was filtered and the remaining red brown product was washed with little acetonitrile and diethyl ether, and finally dried *in vacuo*. Yield: 6.92 g (11.39 mmol, 84 %). **Elemental analysis** $C_{21}H_{28}BN_6O_3W$ (607.14 g mol^{-1}): C 41.13 (calcd. 41.54), H 4.99 (4.65), N 13.97 (13.84) %. **IR** (ATR, cm^{-1}): $\tilde{\nu}$ = 2540 (w, BH), 1966 (s, CO), 1831 (s, CO).

III. Tp*W(CO)(I)(HC≡CH) 1a

A solution of Tp*W(CO)$_3$ (6.39 g, 10.50 mmol) in 180 mL CH_2Cl_2 was purged for 10 min with pure C_2H_2. Solid [(C$_5$H$_5$)$_2$Fe][PF$_6$] (3.48 g, 10.0 mmol) was added in small portions within 60 min continuously purging with a moderate flow of C_2H_2. After additional 30 min the C_2H_2 flow was stopped and the army green solution was further stirred until *in situ* IR confirmed the complete formation of [Tp*W(CO)$_2$(C$_2$H$_2$)]$^+$ [$\tilde{\nu}$ = 2569 (w, BH), 2081, 1907 (s, CO)]. All volatiles were removed *in vacuo* and the resulting green residue was washed with diethyl ether (3 x 20 mL). A suspension of [NBu$_4$]I (6.78 g, 18.35 mmol) in 200 mL THF was added all at once and the black solution was stirred for 60 min. Again *in situ* IR was used to check the progress of the reaction until all [Tp*W(CO)$_2$(C$_2$H$_2$)][PF$_6$] had reacted. After the solvent was removed *in vacuo*, 100 mL methanol were added and the resulting brown suspension was filtered yielding a dull green solid. The crude product was washed several times with methanol and finally dried in air. Yield: 4.51 g (6.41 mmol, 61 %). **Elemental analysis** $C_{21}H_{30}BIN_6OW$ (704.06 g mol^{-1}): C 35.35 (calcd. 35.82), H 4.21 (4.29), N 11.62 (11.94) %. **^{1}H NMR** (CDCl$_3$, 300 MHz, 300 K): δ = 13.56 (d, ^3J = 0.57 Hz, 1 H, CH_{syn}), 12.36 (d, ^3J = 0.57 Hz, 1 H, CH_{anti}), 2.73 (s, 3 H, CCH_3), 2.62 (s, 3 H, CCH_3), 2.49 (s, 3 H, CCH_3), 2.36 (s, 3 H, CCH_3), 2.27 (s, 3 H, CCH_3), 2.01 (s, 3 H, CCH_3), 1.83 (s, 3 H, CCH_3), 1.72 (s, 3 H, CCH_3), 1.65 (s, 3 H, CCH_3) ppm. **^{13}C NMR** ($CDCl_3$, 75 MHz, 300 K): δ = 231.1 (W*C*O), 208.3 (WC_{anti}), 198.1 (WC_{syn}), 153.5, 152.6, 147.1, 143.2, 141.9, 140.7, 113.9, 113.3, 112.7 (*C*CH_3), 17.1, 16.8, 14.4, 11.1, 10.9, 10.8, 8.5, 8.3, 8.2 (CCH_3) ppm. **IR** (THF, cm^{-1}): $\tilde{\nu}$ = 2552 (w, BH), 1914 (vs, CO); (ATR, cm^{-1}): $\tilde{\nu}$ = 2543 (w, BH), 1886 (vs, CO).

IV. Tp*W(CO)(CN)(HC≡CH) 1b

Solid **1a** (1.24 g, 1.76 mmol) and AgCN (0.329°g, 2.46 mmol) were suspended in in 80 mL ethyl acetate in a thick-walled glass flask fitted with a Young valve. After several freeze/pump cycles the closed flask was carefully heated under vacuum for 16°h in a 130 °C hot oil bath during which the colour changed from green to a brownish grey. After cooling down to room temperature, the solvents were removed *in vacuo* leaving a dark brown mixture. Chromatography on silica with a 5:1:1 mixture of CH_2Cl_2, diethyl ether and petroleum ether yielded a green band first, which was identified as unreacted **1a** (219 mg, 18 %), before a bright blue band of **1b** was eluted. Single Crystals suitable for XRD analysis could be obtained by slow diffusion of *n*-pentane into a concentrated solution of **1b** in CH_2Cl_2. Yield: 606 mg (1.01 mmol, 58 %) **Elemental analysis** $C_{22}H_{30}BN_7OW$ (603.17 g mol^{-1}): C 43.15 (calcd. 43.81), H 4.98 (5.01), N 16.03 (16.26) %. **^{1}H NMR** ($CDCl_3$, 250 MHz, 300 K): δ = 13.66 (s, 1 H, CH_{syn}), 12.71 (s, 1 H, CH_{anti}), 2.73 (s, 3 H, CCH_3), 2.49 (s, 3 H, CCH_3), 2.46 (s, 3 H, CCH_3), 2.37 (s, 3 H, CCH_3), 2.28 (s, 3 H, CCH_3), 2.00 (s, 3 H, CCH_3), 1.86 (s, 3 H, CCH_3), 1.76 (s, 3 H, CCH_3), 1.60 (s, 3 H, CCH_3) ppm. **^{13}C NMR** ($CDCl_3$, 63 MHz, 300 K): δ = 228.6 (W*C*O), 213.8 (WC_{anti}), 204.1 (WC_{syn}), 153.1, 151.9 (*C*CH_3), 151.5 (*C*N), 146.4, 143.2, 142.6, 141.0, 113.6, 113.2, 112.9 (*C*CH_3), 15.5, 14.9, 14.2, 11.1, 10.8, 10.8, 8.4, 8.2, 8.1 (CCH_3) ppm. **IR** (THF, cm^{-1}): $\tilde{\nu}$ = 2552 (w, BH), 2116 (w, CN), 1926 (vs, CO); (ATR, cm^{-1}): $\tilde{\nu}$ = 2553 (w, BH), 2113 (m, CN), 1903 (vs, CO).

V. Tp*W(CO)(I)(Ph$_2$PC≡CH) 2a

A blue green solution of **1a** (1 g, 1.42 mmol) in 190 mL THF was cooled to -78 °C for 30 min, before adding *n*-butyllithium (2.5 M solution in *n*-hexane, 0.74 mL) dropwise. The resulting black solution was stirred for 30 min at -78 °C to complete the reaction. After adding $ClPPh_2$ (0.42 mL, 2.27 mmol) the solution turned green and was allowed to warm up. At room temperature the volatiles were removed *in vacuo* leaving a green residue, which was purified by column chromatography on silica using a 1:1 mixture of petroleum ether and CH_2Cl_2. A blue band was eluted. The solvents were removed yielding a blue powder. Single Crystals suitable for XRD analysis could be obtained by slow diffusion of *n*-pentane into a concentrated solution of **2a** in CH_2Cl_2. Yield: 1.03 g (1.16 mmol, 82 %). **Elemental analysis** $C_{33}H_{39}BIN_6OPW\cdot 0.5\ C_5H_{12}$ (924.31 g mol^{-1}): C 46.63 (calcd. 46.13), H 4.89 (4.91), N 8.82 (9.09) %. **^{1}H NMR** ($CDCl_3$, 300 MHz, 300 K): δ = 13.44 (s, 1 H, CH_{syn}), 7.31–7.14 (m, 6 H, Ph-*H*), 6.90 (m, 2 H, Ph-*H*), 6.38 (m, 2 H, Ph-*H*), 2.73 (s, 3 H, CCH_3), 2.54 (s, 3 H, CCH_3), 2.41 (d, J_{HP} = 1.5 Hz, 3 H, CCH_3), 2.26 (s, 3 H, CCH_3), 2.22 (s, 3 H, CCH_3), 1.80 (s, 3 H, CCH_3), 1.75 (s, 3 H, CCH_3), 1.50 (s, 3 H, CCH_3), 1.15 (s, 3 H, CCH_3) ppm. **^{13}C NMR** ($CDCl_3$, 75 MHz, 300 K): δ = 232.2 (d, $^3J_{CP}$ = 3.9 Hz, W*C*O), 212.6 (d, $^1J_{CP}$ = 55.5 Hz, W*C*$_{anti}$), 207.2 (d, $^2J_{CP}$ = 3.9 Hz, W*C*$_{syn}$), 153.2, 152.5, 146.8, 142.6, 141.7, 140.2 (*C*CH$_3$), 139.6, 139.4 (*C*$_{ipso}$), 134.9–127.3 (Ph-*C*, 10 signals), 113.1, 113.1, 112.8 (*C*CH$_3$), 18.8 (d, J_{CP} = 15.4 Hz, C*C*H$_3$), 16.8, 13.4, 11.1, 10.9, 10.6, 8.4, 8.2, 8.2 (C*C*H$_3$) ppm. **^{31}P{H} NMR** (CDCl$_3$, 121 MHz, 300 K): δ = 18.4 ppm. **IR** (THF, cm^{-1}): $\tilde{\nu}$ = 2554 (w, BH), 1917 (vs, CO); (ATR, cm^{-1}): $\tilde{\nu}$ = 2557 (w, BH), 1898 (vs, CO).

VI. Tp*W(CO)(CN)(Ph$_2$PC≡CH) 2b

Complex **2b** was obtained analogous to **2a** using **1b** (700 mg, 1.16 mmol) instead of **1a** and a 5:2 mixture of CH$_2$Cl$_2$ and diethyl ether as eluent in the chromatographic purification to isolate a blue-green band. Single Crystals suitable for XRD analysis could be obtained by slow diffusion of *n*-pentane into a concentrated solution of **2b** in CH$_2$Cl$_2$. Yield: 448 mg (0.569 mmol, 49 %). **Elemental analysis** C$_{34}$H$_{39}$BN$_7$OPW (787.35 g mol^{-1}): C 51.63 (calcd. 51.87), H 4.88 (4.99), N 12.45 (12.42) %. **^{1}H NMR** (CDCl$_3$, 300 MHz, 300 K): δ = 13.47 (s, 1 H, C*H*$_{syn}$), 7.31–7.11 (m, 6 H, Ph-*H*), 6.86 (m, 2 H, Ph-*H*), 6.46 (m, 2 H, Ph-*H*), 2.73 (s, 3 H, CC*H$_3$*), 2.49 (s, 3 H, CC*H$_3$*), 2.31 (d, J_{HP} = 1.1 Hz, 3 H, CC*H$_3$*), 2.20 (s, 3 H, CC*H$_3$*), 2.19 (s, 3 H, CC*H$_3$*), 1.81 (s, 3 H, CC*H$_3$*), 1.78 (s, 3 H, CC*H$_3$*), 1.52 (s, 3 H, CC*H$_3$*), 1.19 (s, 3 H, CC*H$_3$*) ppm. **^{13}C NMR** (CDCl$_3$, 75 MHz, 300 K): δ = 230.0 (d, $^3J_{CP}$ = 3.2 Hz, W*C*O), 219.7 (d, $^1J_{CP}$ = 54.6 Hz, W*C*$_{anti}$), 210.6 (d, $^2J_{CP}$ = 4.8 Hz, W*C*$_{syn}$), 152.8 (d, $^2J_{CP}$ = 1.6 Hz, *C*N), 152.5, 151.8, 146.1, 142.7, 142.6, 140.6 (*C*CH$_3$), 139.2, 139.1 (*C*$_{ipso}$), 134.5–127.4 (Ph-*C*, 10 signals), 113.1, 112.9, 112.8 (*C*CH$_3$), 15.6 (d, J_{CP} = 14.5 Hz, C*C*H$_3$), 14.9, 13.6, 11.2, 10.9, 10.5, 8.3, 8.1, 8.1 (C*C*H$_3$) ppm. **^{31}P{H} NMR** (CDCl$_3$, 121 MHz, 300 K): δ = 15.9 ppm. **IR** (THF, cm^{-1}): $\tilde{\nu}$ = 2551 (w, BH), 2113 (w, CN), 1926 (vs, CO); (ATR, cm^{-1}): $\tilde{\nu}$ = 2546 (w, BH), 2111 (w, CN), 1915 (vs, CO).

VII. Tp*W(CO)(I)(Ph$_2$PC≡CPPh$_2$) 3a

A blue solution of **2a** (1.2 g, 1.35 mmol) in 120 mL THF was cooled to -78 °C for 15 min, before adding *n*-butyllithium (2.5 M solution in *n*-hexane, 0.8 mL) dropwise. The resulting dark blue solution was stirred for 30 min at -78 °C to complete the reaction. After adding ClPPh$_2$ (0.42 mL, 2.27 mmol) the solution turned green and was allowed to warm up. At room temperature, the volatiles were removed *in vacuo* leaving a green residue, which was purified by column chromatography on silica. A bright green band was eluted with toluene. The solvent was removed yielding a green powder. Single Crystals suitable for XRD analysis could be obtained by slow diffusion of *n*-pentane into a concentrated solution of **3a** in CH$_2$Cl$_2$. Yield: 1.22 g (1.14 mmol, 84 %). **Elemental analysis** C$_{45}$H$_{48}$BN$_6$OP$_2$W (1072.41 g mol^{-1}): C 50.30 (calcd. 50.40), H 4.45 (4.51), N 7.83 (7.84) %. **^{1}H NMR** (CDCl$_3$, 250 MHz, 300 K): δ = 8.09 (m, 2 H, Ph-*H*), 7.44–6.98 (m, 12 H, Ph-*H*), 6.78 (m, 2 H, Ph-*H*), 6.59 (m, 2 H, Ph-*H*), 6.46 (m, 2 H, Ph-*H*), 2.56 (s, 3 H, CC*H$_3$*), 2.54 (s, 3 H, CC*H$_3$*), 2.51 (d, J_{HP} = 1.9 Hz, 3 H, CC*H$_3$*), 2.19 (s, 3 H, CC*H$_3$*), 2.15 (s, 3 H, CC*H$_3$*), 2.08 (s, 3 H, CC*H$_3$*), 1.93 (s, 3 H, CC*H$_3$*), 1.74 (s, 3 H, CC*H$_3$*), 1.49 (s, 3 H, CC*H$_3$*) ppm. **^{13}C NMR** (CDCl$_3$, 62 MHz, 300 K): δ = 233.3 (pseudo-t, $^3J_{CP}$ = 2.7 Hz, W*C*O), 222.4 (dd, $^1J_{CP}$ = 52.0 Hz, $^2J_{CP}$ = 5.4 Hz W*C*$_{anti}$), 213.2 (dd, $^1J_{CP}$ = 48.6 Hz, $^2J_{CP}$ = 4.6 Hz, W*C*$_{syn}$), 153.1, 152.6 (*C*CH$_3$), 150.5 (d, J_{CP} = 1.5 Hz, *C*CH$_3$), 143.4, 141.5, 140.3 (*C*CH$_3$), 137.5, 137.4 (*C*$_{ipso}$), 137.2, 136.9 (Ph-*C*, 2 signals), 136.7, 136.7 (C_{ipso}), 135.5–127.0 (Ph-*C*, 18 signals), 113.6, 113.3, 113.2 (*C*CH$_3$), 20.0 (d, J_{CP} = 18.5 Hz, C*C*H$_3$), 17.4 (C*C*H$_3$), 15.2 (d, J_{CP} = 11.6 Hz, C*C*H$_3$), 11.3, 11.2, 10.7, 8.7, 8.4, 8.3 (C*C*H$_3$) ppm. **^{31}P{H} NMR** (CDCl$_3$, 121 MHz, 300 K): δ = 20.0 (d, $^3J_{PP}$ = 10.4 Hz), 18.1 (d, $^3J_{PP}$ = 10.4 Hz) ppm. **IR** (THF, cm^{-1}): $\tilde{\nu}$ = 2554 (w, BH), 1933 (vs, CO); (CH$_2$Cl$_2$, cm^{-1}): $\tilde{\nu}$ = 2559 (w, BH), 1930 (vs, CO); (ATR, cm^{-1}): $\tilde{\nu}$ = 2559 (w, BH), 1913 (vs, CO).

VIII. Tp*W(CO)(CN)(Ph$_2$PC≡CPPh$_2$) 3b

Complex **3b** was obtained analogous to **3a** using **2b** (360 mg, 0.457 mmol) instead of **2a** and a 5:1:1 mixture of CH$_2$Cl$_2$, diethyl ether and petroleum ether as eluent in the chromatography to isolate a green band. The solvent was removed yielding a green powder. Single Crystals suitable for XRD analysis could be obtained by layering a concentrated solution of **3b** in CH$_2$Cl$_2$ with *n*-pentane. Yield: 320 mg (0.329 mmol, 72 %). **Elemental analysis** $C_{46}H_{48}BN_7OP_2W$ (971.52 g mol^{-1}): C 56.84 (calcd. 56.87), H 5.00 (4.98), N 9.69 (10.09) %. **^{1}H NMR** (CDCl$_3$, 300 MHz, 300 K): δ = 8.12 (m, 2 H, Ph-*H*), 7.55–6.96 (m, 12 H, Ph-*H*), 6.76 (m, 2 H, Ph-*H*), 6.64 (m, 2 H, Ph-*H*), 6.54 (m, 2 H, Ph-*H*), 2.58 (s, 3 H, CC*H$_3$*), 2.53 (s, 3 H, CC*H$_3$*), 2.46 (d, J_{HP} = 1.5 Hz, 3 H, CC*H$_3$*), 2.17 (s, 3 H, CC*H$_3$*), 2.11 (s, 3 H, CC*H$_3$*), 2.05 (s, 3 H, CC*H$_3$*), 1.95 (s, 3 H, CC*H$_3$*), 1.77 (s, 3 H, CC*H$_3$*), 1.56 (s, 3 H, CC*H$_3$*) ppm. **^{13}C NMR** (CDCl$_3$, 75 MHz, 300 K): δ = 231.2 (pt, $^3J_{CP}$ = 3.6 Hz, W*C*O), 227.2 (dd, $^1J_{CP}$ = 50.0 Hz, $^2J_{CP}$ = 7.3 Hz WC_{anti}), 216.2 (dd, $^1J_{CP}$ = 45.4 Hz, $^2J_{CP}$ = 6.4 Hz, WC_{syn}), 154.3 (br, *C*N), 152.2, 151.7 (*C*CH$_3$), 149.3 (d, J_{CP} = 1.8 Hz, *C*CH$_3$), 143.3, 142.4, 140.5 (*C*CH$_3$), 137.4, 137.3, 136.5, 136.5 (C_{ipso}), 135.8 (Ph-*C*), 134.2–133.2 (Ph-*C*, 11 signals), 129.8–127.0 (Ph-*C*, 8 signals), 113.5, 113.0, 112.9 (*C*CH$_3$), 16.3 (d, J_{CP} = 16.4 Hz, C*C*H$_3$), 15.1 (C*C*H$_3$), 14.7 (d, J_{CP} = 7.3 Hz, C*C*H$_3$), 11.1, 11.0, 10.5, 8.4, 8.2, 8.1 (C*C*H$_3$) ppm. **^{31}P{H} NMR** (CDCl$_3$, 121 MHz, 300 K): δ = 16.7 (d, $^3J_{PP}$ = 10.4 Hz), 16.3 (d, $^3J_{PP}$ = 10.4 Hz) ppm. **IR** (THF, cm^{-1}): $\tilde{\nu}$ = 2551 (w, BH), 2110 (w, CN), 1939 (vs, CO); (CH$_2$Cl$_2$, cm^{-1}): $\tilde{\nu}$ = 2557 (w, BH), 2109 (w, CN), 1939 (vs, CO); (ATR, cm^{-1}): $\tilde{\nu}$ = 2554 (w, BH), 2104 (m, CN), 1934 (vs, CO).

IX. [Tp*W(CO)(I){Ph$_2$PC≡CPPh$_2$}][A] 3a-A, A = BF$_4$, PF$_6$

[(C$_5$H$_5$)Fe{C$_5$H$_4$C(O)CH$_3$}][A] (A = BF$_4$: 29.4 mg, 0.093 mmol; PF$_6$: 17.3 mg, 0.046 mmol) and **3a** (A = BF$_4$: 100 mg, 0.093 mmol; PF$_6$: 50 mg, 0.046 mmol) were mixed in a Schlenk flask as solids. Addition of 5 mL CH$_2$Cl$_2$ immediately led to a dark red solution, which was cooled down to -40 °C after 1 min of stirring. The solution was concentrated *in vacuo* at -40 °C and recrystallization from CH$_2$Cl$_2$/diethyl ether at -25 °C yielded the product as a dark red microcrystalline material. It can be stored in the fridge for several days, but decomposes rapidly at room temperature. Single crystals suitable for XRD analysis could be obtained by layering a concentrated solution of pure **3a**-PF$_6$ in CH$_2$Cl$_2$ with an excess *n*-pentane performed at -25 °C. Yield: A = BF$_4$ 78 mg (0.067 mmol, 72 %); A = PF$_6$ 31 mg (0.025 mmol, 55 %). **Elemental analysis** (bulk, **3a**-BF$_4$) $C_{45}H_{48}B_2F_4N_6OP_2W$ (1159.21 g mol^{-1}): C 46.60 (calcd. 46.62), H 4.25 (4.17), N 7.15 (7.25) %. **IR** (CH$_2$Cl$_2$, cm^{-1}): $\tilde{\nu}$ = 2573 (w, BH), 2079 (vs, CO); (ATR, cm^{-1}): $\tilde{\nu}$ = 2572 (w, BH), 2069 (s, CO).

X. [Tp*W(CO)(I){$Ph_2P(NH_2)C{\equiv}CP(O)Ph_2$}][$BF_4$] 4a-$BF_4$

Method A. Freshly prepared **3a**-BF_4 (70 mg, 0.06 mmol) was dissolved at -40 °C in 10 mL of pre-cooled CH_2Cl_2, before an excess of NO gas was passed through the stirred solution. After 5 min the gas flow was stopped and the solution was allowed to warm up as IR spectroscopy indicated full conversion. The volatiles were removed *in vacuo* and the crude red product was recrystallized several times from CH_2Cl_2/diethyl ether. Yield 52 mg (0.044 mmol, 71 %).

Method B. [NO][BF_4] (10.5 mg, 0.093 mmol) and **3a** (100 mg, 0.093 mmol) were mixed in a Schlenk flask as solids. Addition of 10 mL CH_2Cl_2 immediately led to a red solution, which was stirred for 45 min until all [NO][BF_4] was consumed. The solvent was removed *in vacuo* and the crude red product was recrystallized several times from CH_2Cl_2/diethyl ether. Single Crystals suitable for XRD analysis could be obtained by slow diffusion of diethyl ether or *n*-pentane into a concentrated solution of **4a**-BF_4 in CH_2Cl_2. Yield: 67 mg (0.056 mmol, 71 %).

Elemental analysis $C_{45}H_{50}B_2F_4N_7O_2P_2W{\cdot}0.5\ C_5H_{12}{\cdot}0.5\ CH_2Cl_2$ (1270.76 g mol^{-1}): C 45.07 (calcd. 44.90), H 4.41 (4.44), N 7.63 (7.72) %. **^{1}H NMR** (CD_2Cl_2, 300 MHz, 300 K): δ = 8.07 (m, 2 H, Ph-*H*), 7.84 (m, 2 H, Ph-*H*), 7.70–7.15 (m, 14 H, Ph-*H*), 6.46 (m, 2 H, Ph-*H*), 5.11 (d, br, J_{HP} = 2.6 Hz, 2 H, NH_2), 2.62 (s, 3 H, CCH_3), 2.62 (s, 3 H, CCH_3), 2.32 (s, 3 H, CCH_3), 2.20 (s, 3 H, CCH_3), 2.04 (s, 3 H, CCH_3), 1.91 (s, 3 H, CCH_3), 1.89 (s, 3 H, CCH_3), 1.75 (s, 3 H, CCH_3), 1.45 (s, 3 H, CCH_3) ppm. **^{13}C NMR** (CD_2Cl_2, 75 MHz, 300 K)*: 154.0, 153.3, 149.6, 146.4, 143.8, 142.6 (*C*CH_3), 135.1–129.0 (Ph-*C*, 24 signals), 115.0, 114.7, 114.7 (*C*CH_3), 19.8, 18.1 16.6, 11.6, 11.4, 11.0, 8.8, 8.6, 8.5 (C*C*H_3) ppm. **^{1}H, ^{15}N HMBC NMR** (CD_2Cl_2, 51 MHz, 300 K): δ = -354 ppm. **^{31}P{H} NMR** (CD_2Cl_2, 121 MHz, 300 K): δ = 36.0 (d, $^3J_{PP}$ = 10.4 Hz), 27.7 (d, $^3J_{PP}$ = 10.4 Hz) ppm. **IR** (CH_2Cl_2, cm^{-1}): $\tilde{\nu}$ = 2568 (w, BH), 1978 (vs, CO); (ATR, cm^{-1}): $\tilde{\nu}$ = 2566 (w, BH), 1955 (vs, CO). **MS** (ESI-TOF, CH_3CN): *m/z* calcd for $C_{45}H_{50}BN_7O_2P_2W^+$: 1104.22 found: 1104.22 [M^+], 1076.22 [M^+–CO].

XI. [Tp*W(CO)(CN){$Ph_2P(NH_2)C{\equiv}CP(O)Ph_2$}][$BF_4$] 4b-$BF_4$

[NO][BF_4] (3.6 mg, 0.031 mmol) and **3b** (30 mg, 0.031 mmol) were mixed in a Schlenk flask as solids. Addition of 6 mL CH_2Cl_2 led to a red solution, which was stirred for until all [NO][BF_4] was consumed. The solvent was removed *in vacuo* and the crude red product was analyzed by ESI-TOF mass spectroscopy.

MS (ESI-TOF, CH_3CN): *m/z* calcd for $C_{46}H_{50}BN_8O_2P_2W^+$: 1003.31 found: 1003.31 [M^+].

* Unfortunately, signals for the quaternary carbon atoms (W*C*O, C*C*P, and C_{ipso}) could not be detected. This observation is attributed to ^{13}C^{31}P coupling and signal broadening due to fluxional behaviour.

2.3 NMR spectra

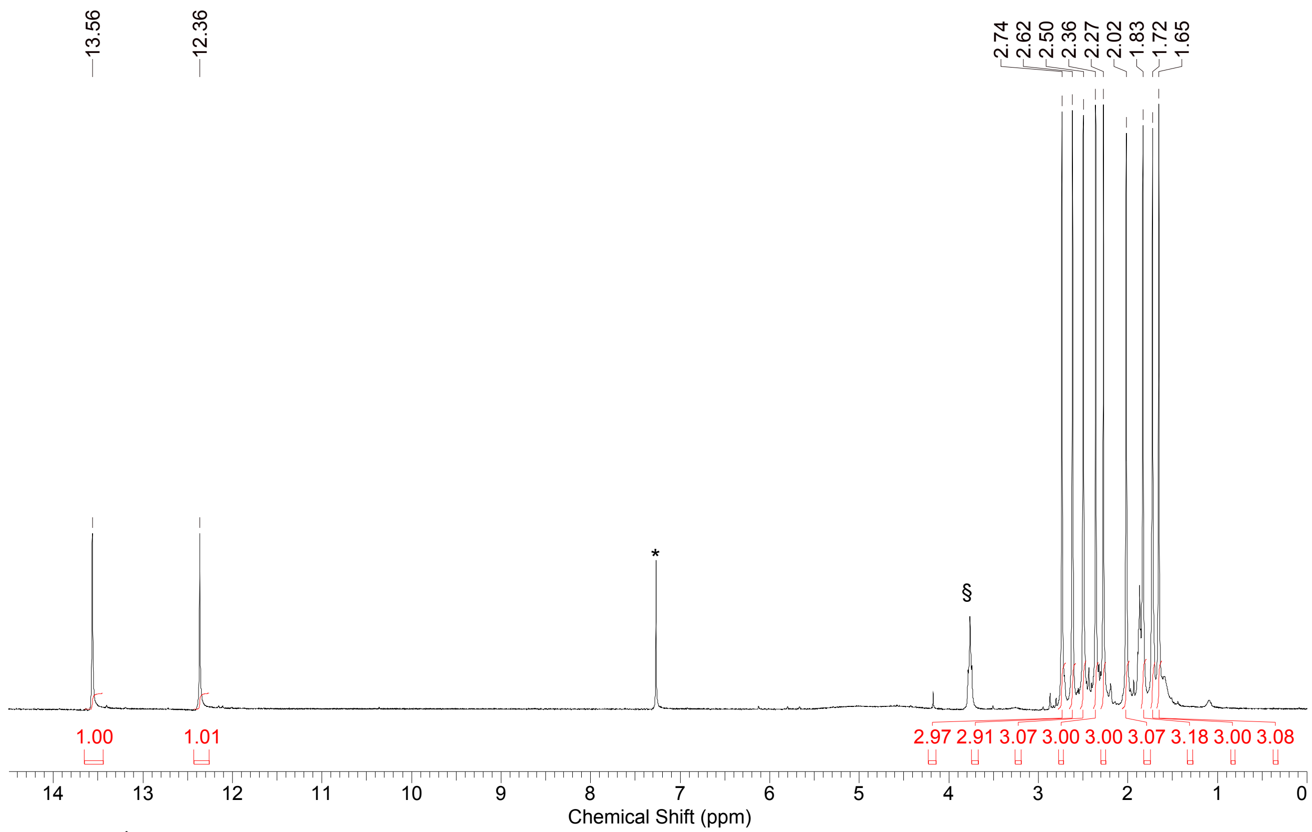

Figure S9. ^{1}H NMR of **1a** in $CDCl_3$ (*). § thf.

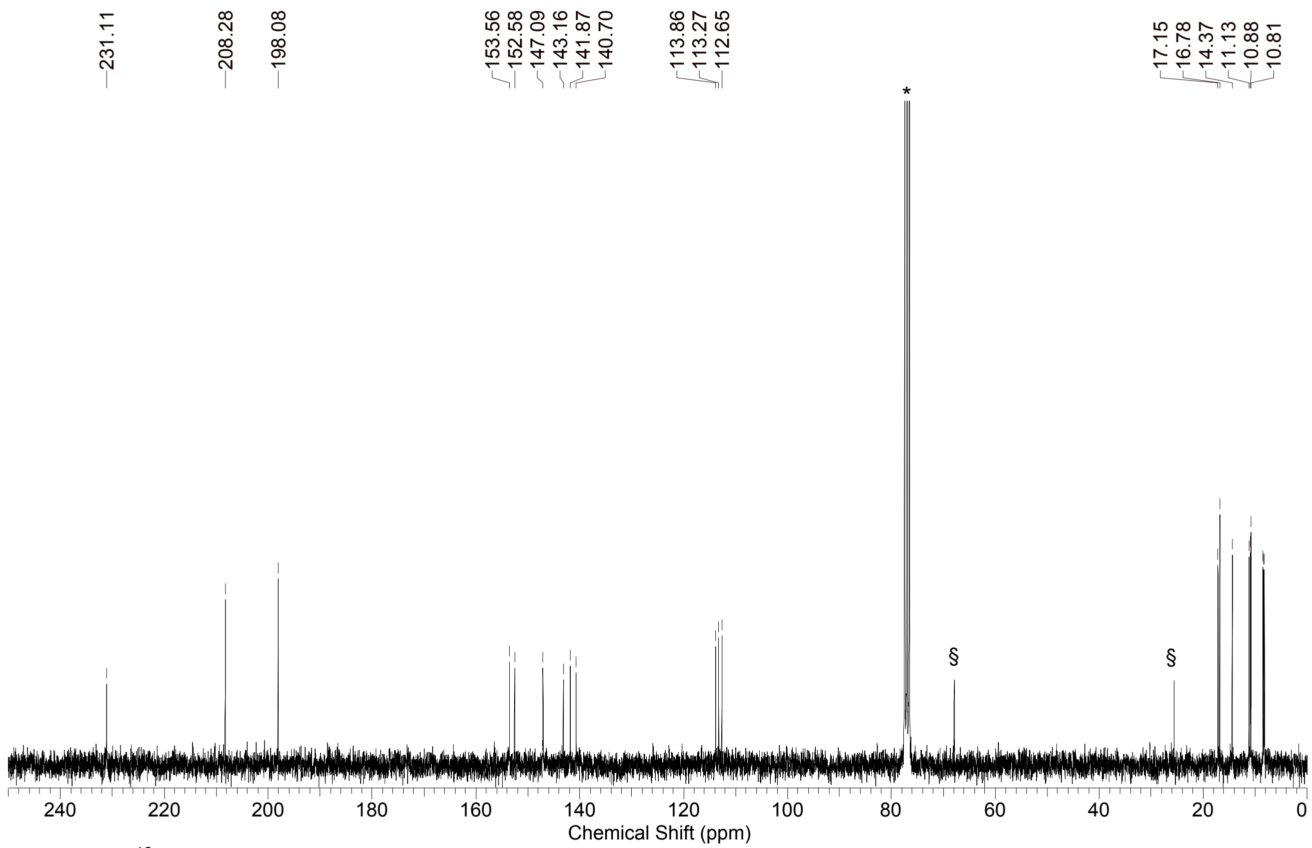

Figure S10. ^{13}C NMR of **1a** in $CDCl_3$ (*). § thf.

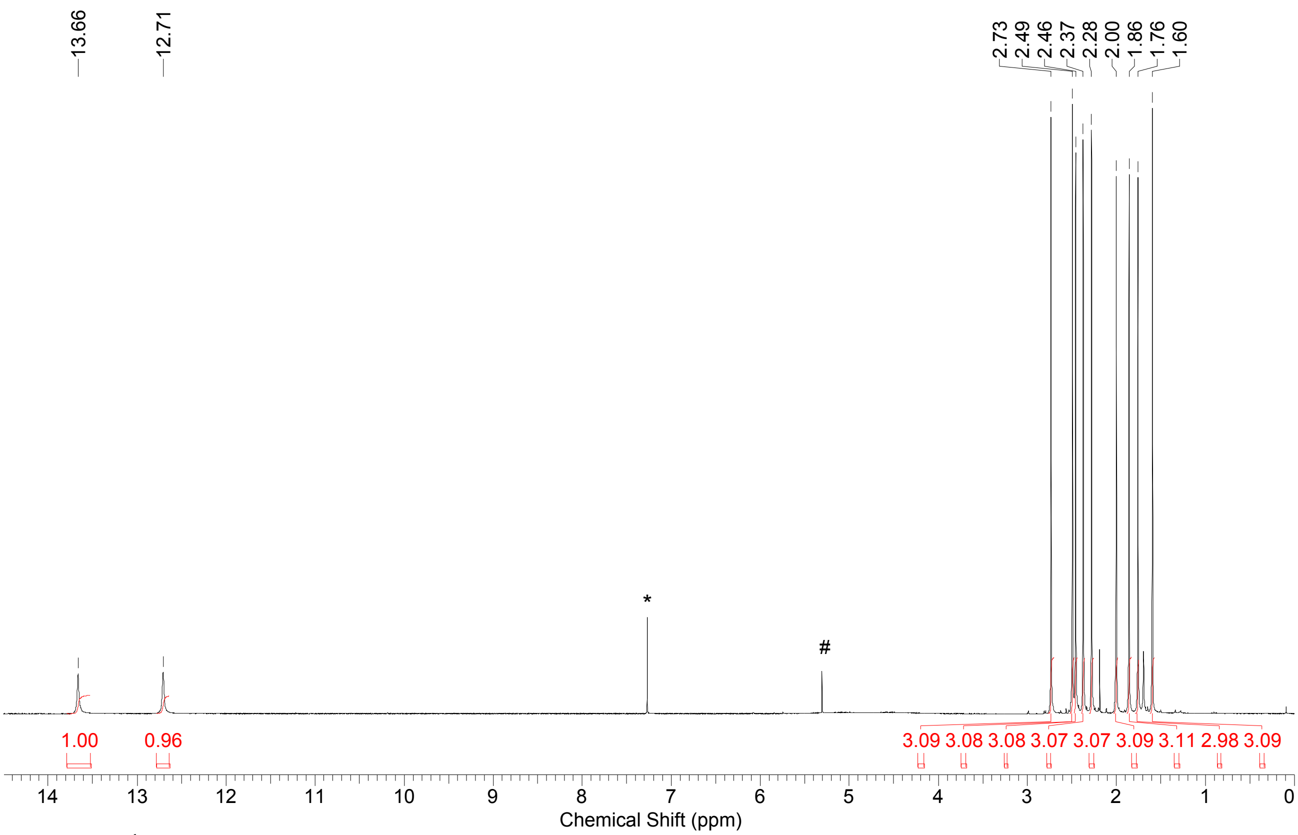

Figure S11. ^{1}H NMR of **1b** in $CDCl_3$ (*). # CH_2Cl_2.

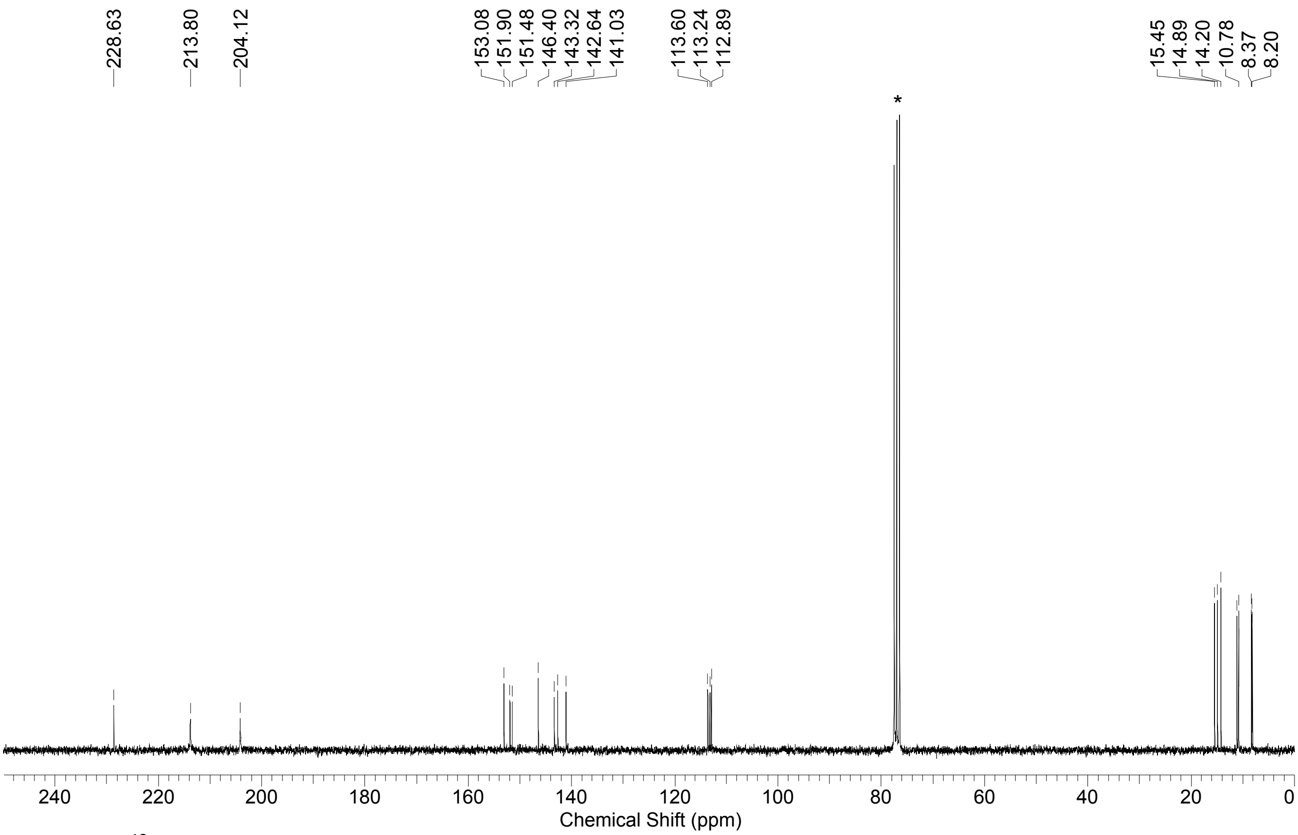

Figure S12. ^{13}C NMR of **1b** in $CDCl_3$ (*).

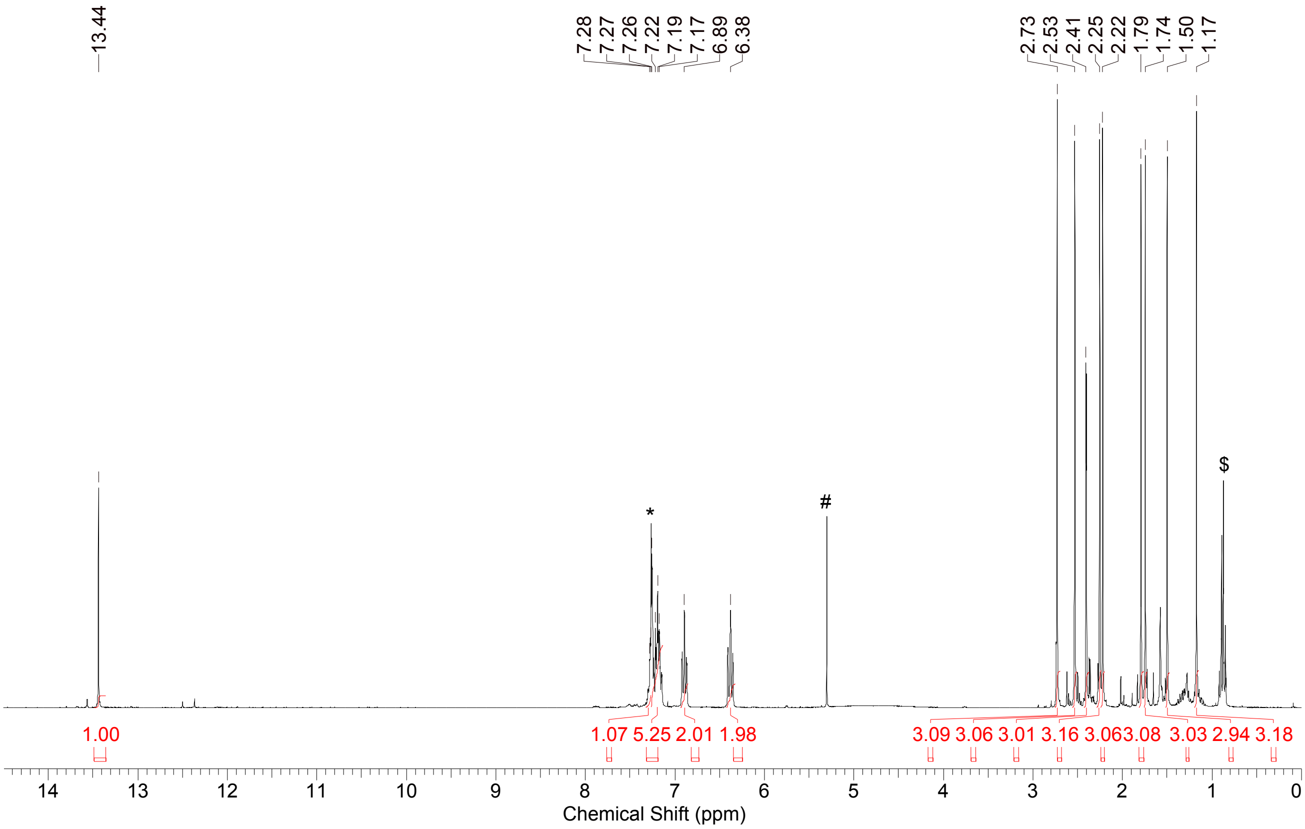

Figure S13. ^{1}H NMR of **2a** in $CDCl_3$ (*). # CH_2Cl_2; $ *n*-pentane.

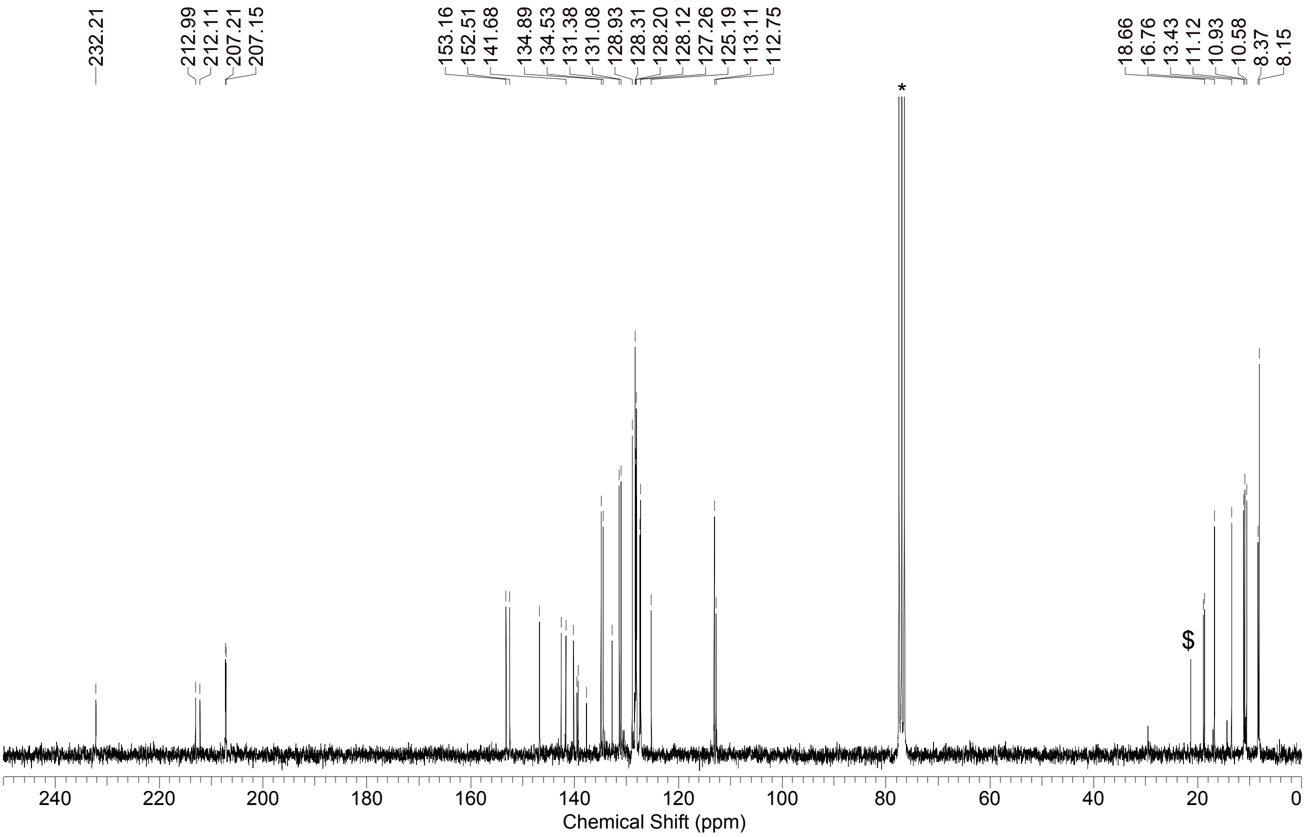

Figure S14. ^{13}C NMR of **2a** in $CDCl_3$ (*). $ *n*-pentane.

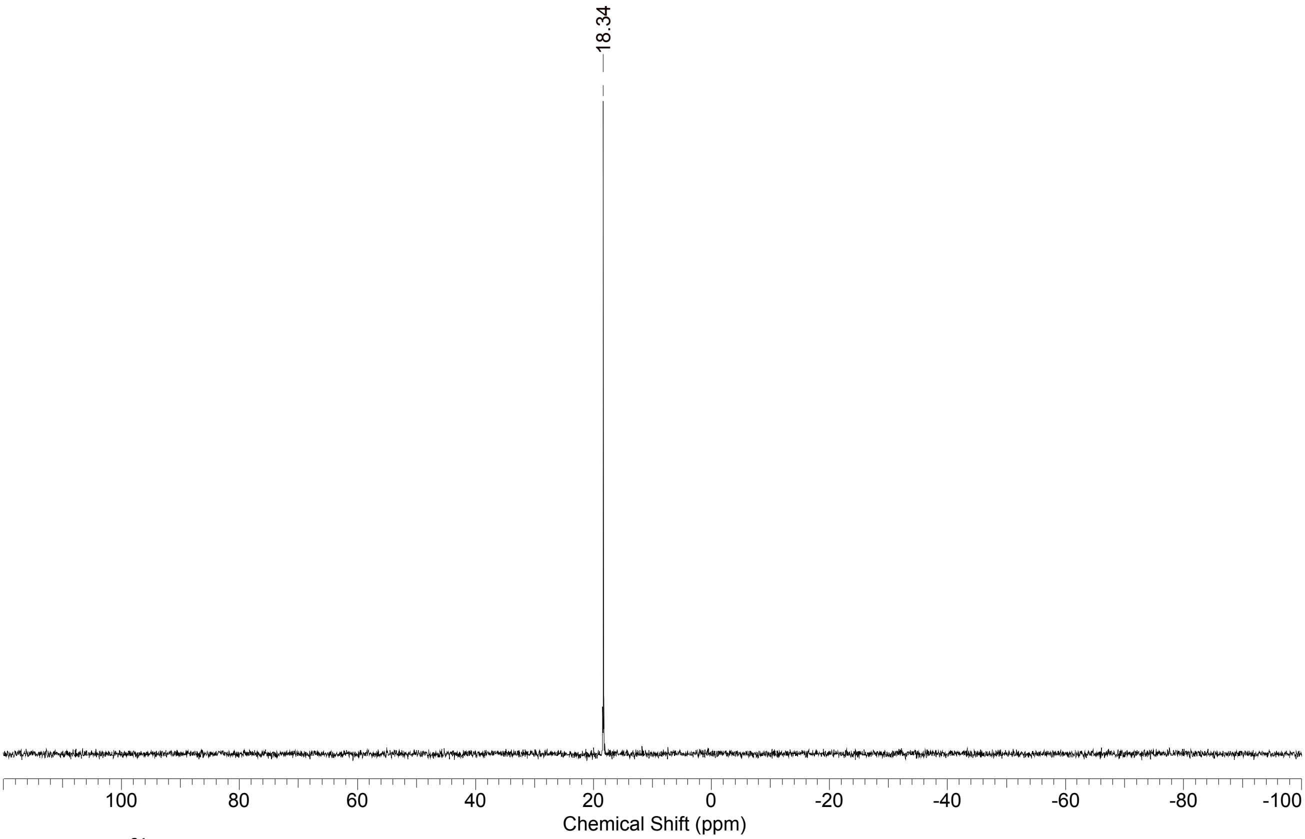

Figure S15. ^{31}P NMR of **2a** in $CDCl_3$.

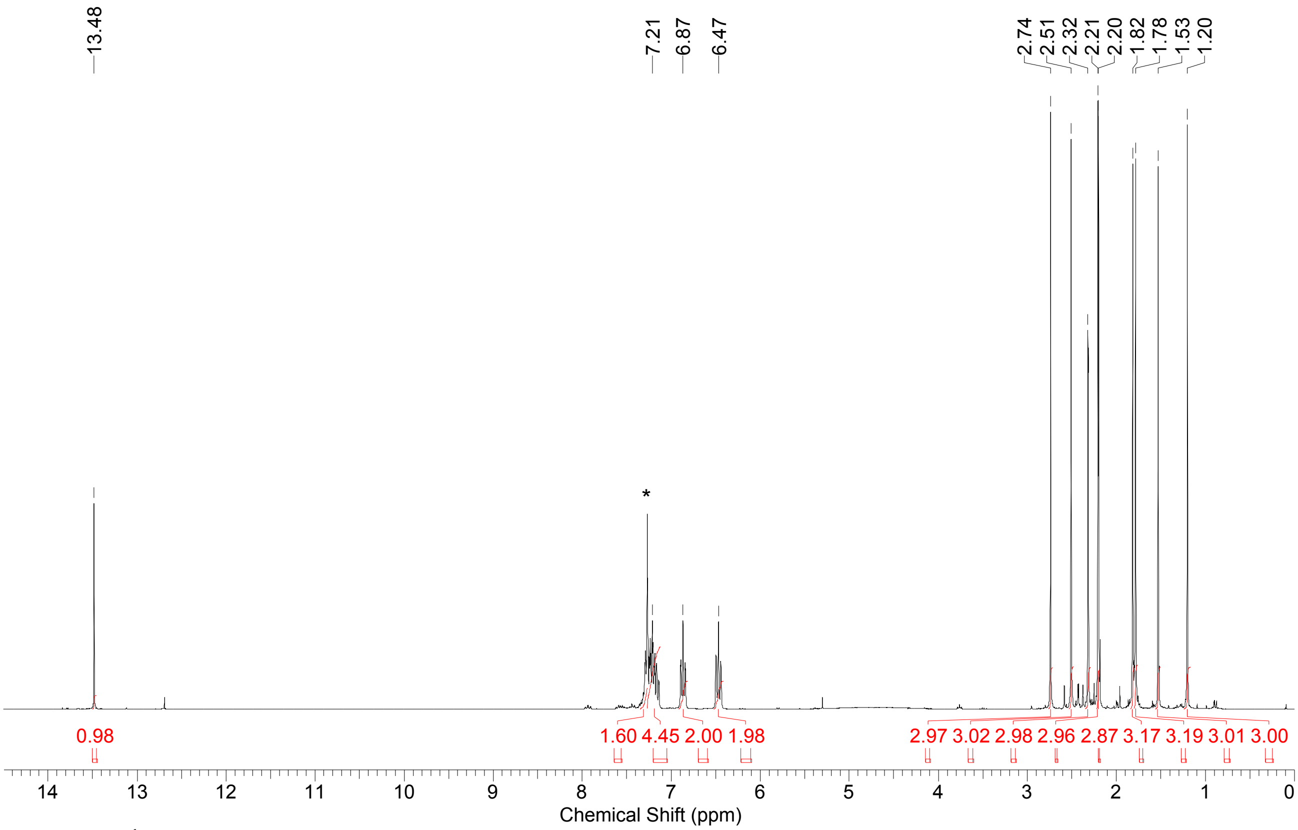

Figure S16. ^{1}H NMR of **2b** in $CDCl_3$ (*).

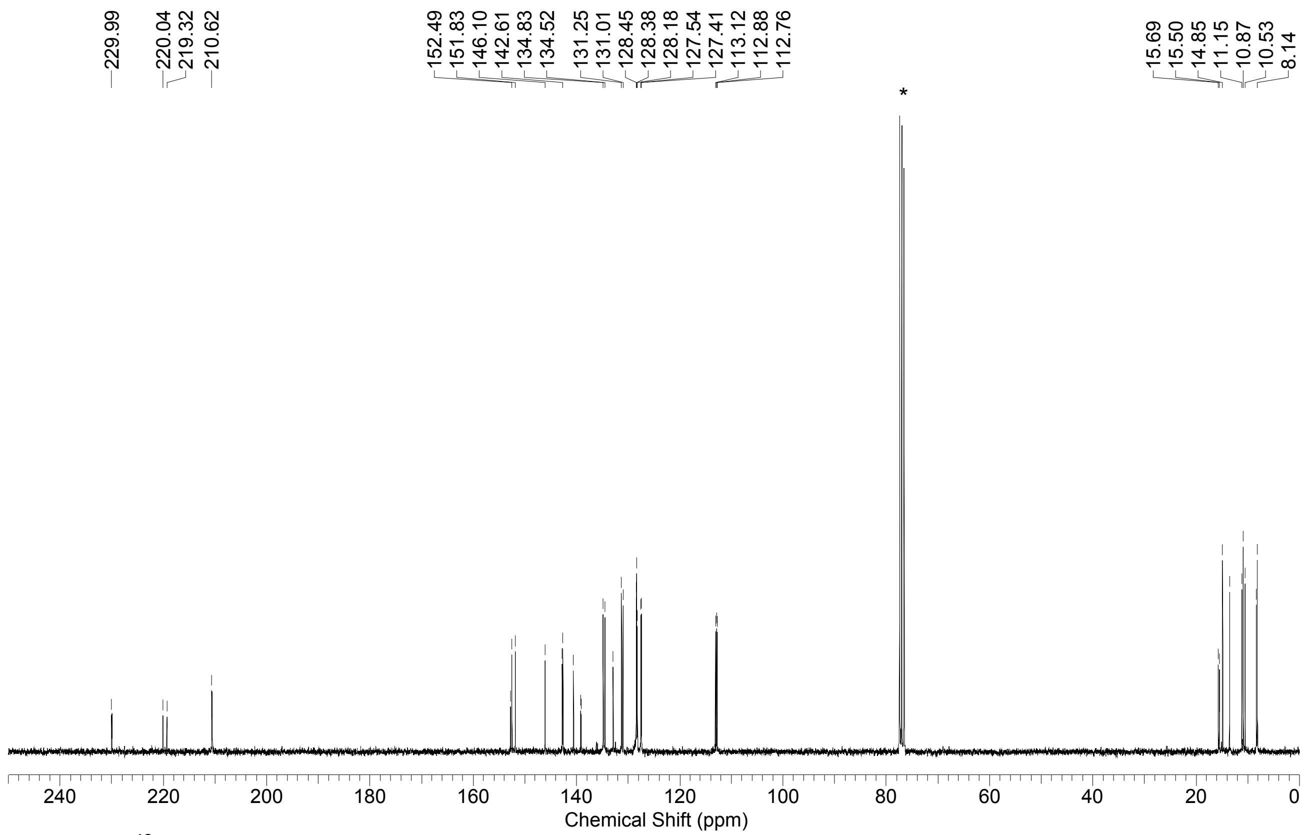

Figure S17. ^{13}C NMR of **2b** in $CDCl_3$ (*).

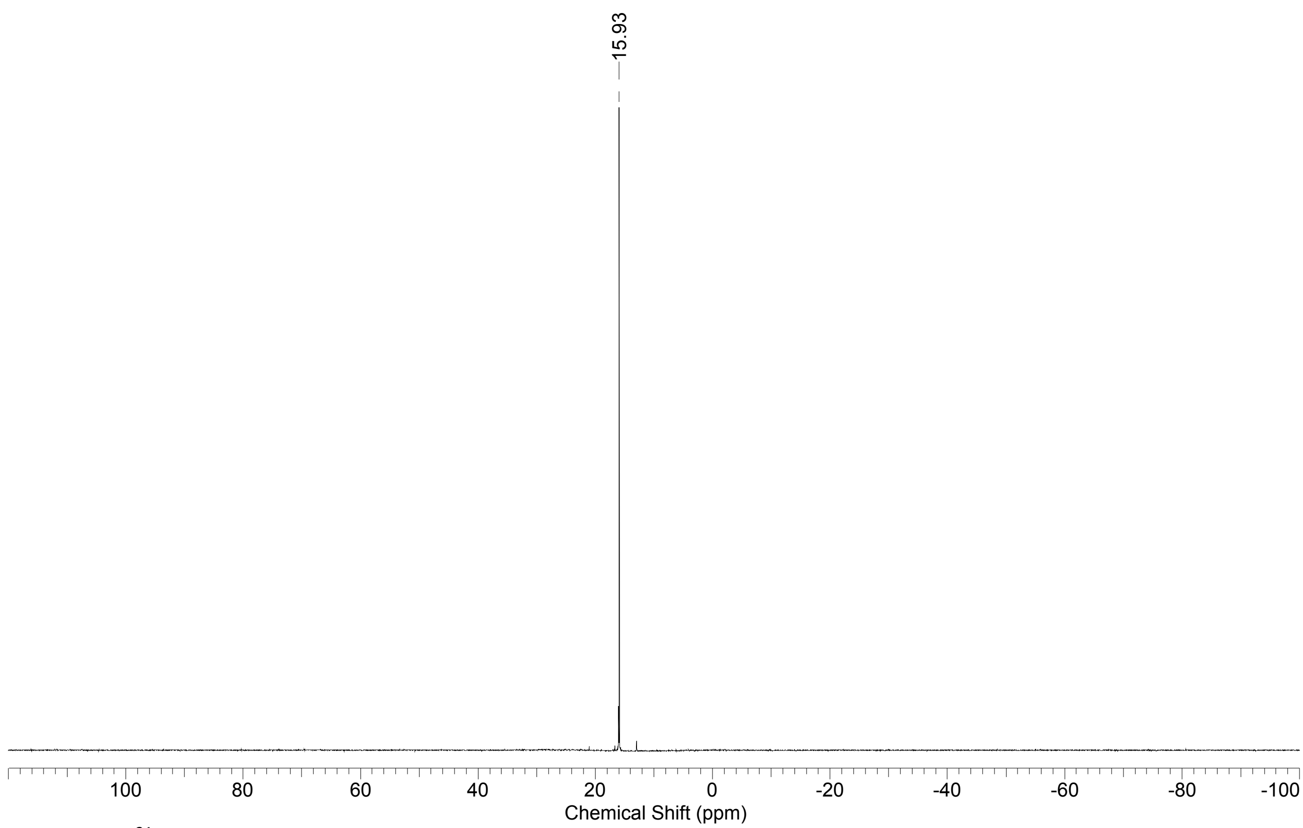

Figure S18. ^{31}P NMR of **2b** in $CDCl_3$.

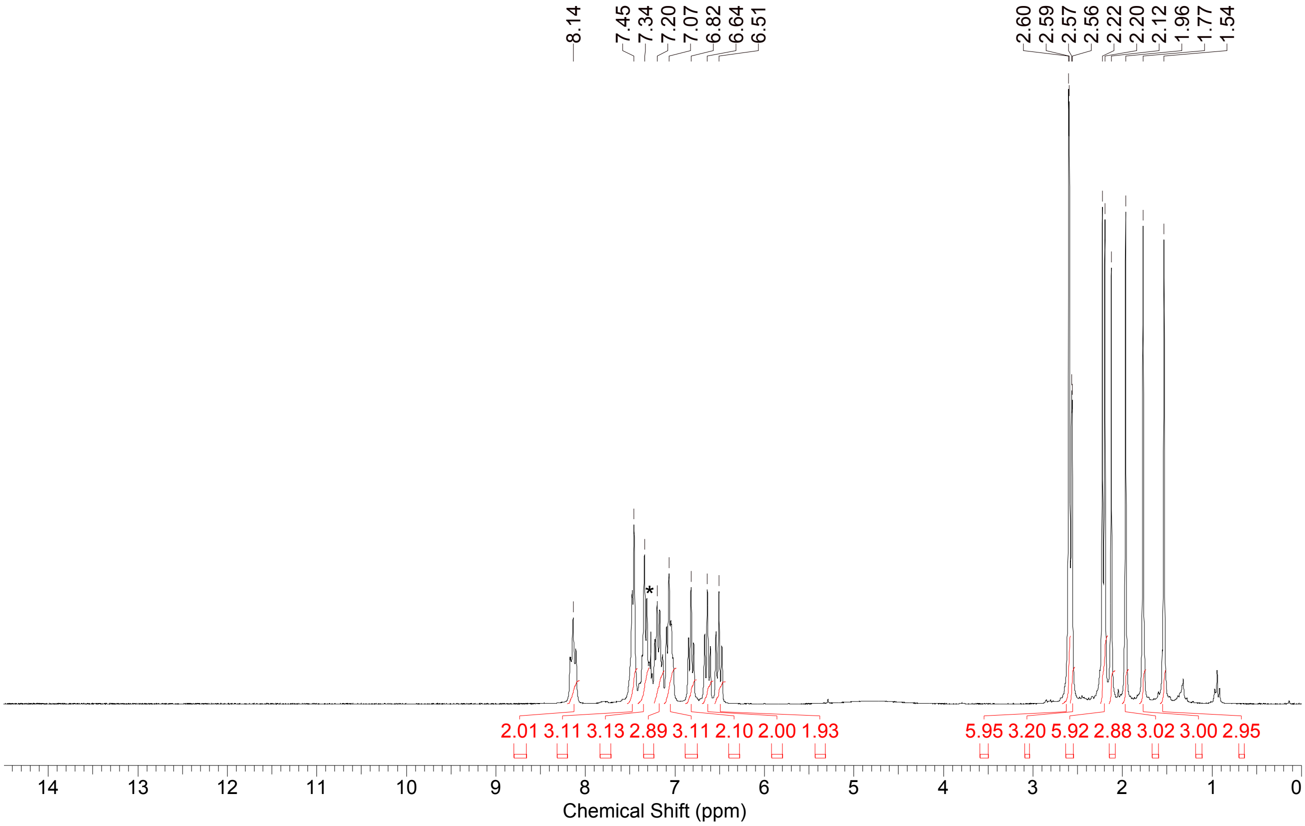

Figure S19. ^{1}H NMR of **3a** in $CDCl_3$ (*).

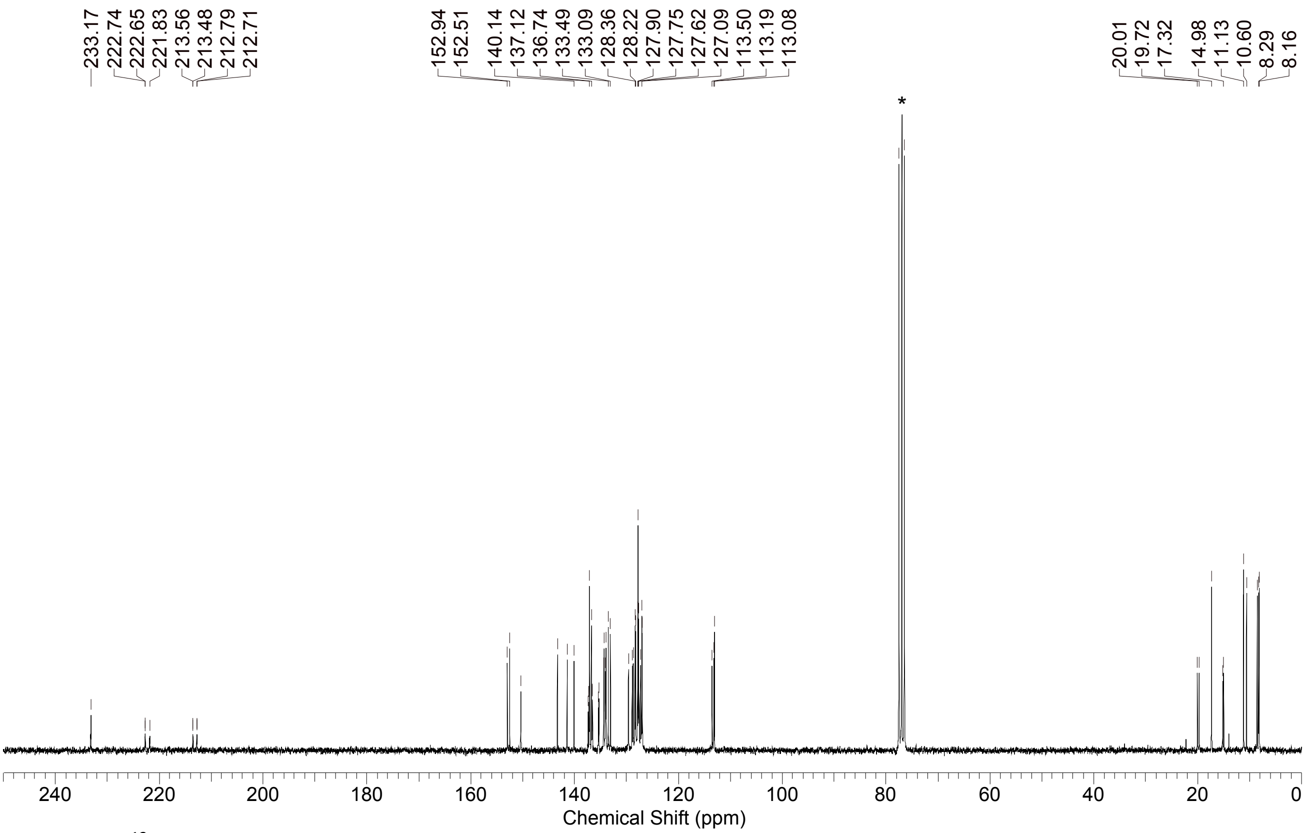

Figure S20. ^{13}C NMR of **3a** in $CDCl_3$ (*).

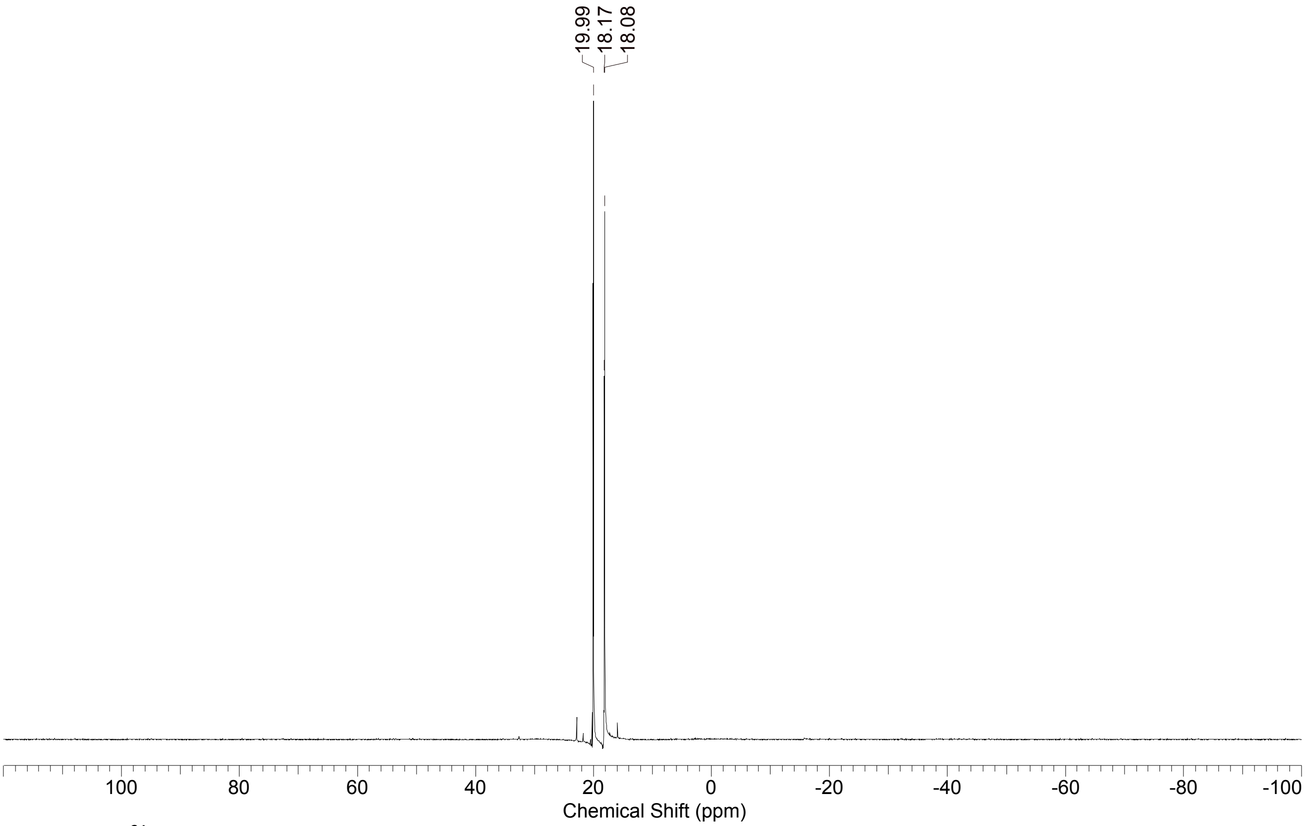

Figure S21. ^{31}P NMR of **3a** in $CDCl_3$ (*)

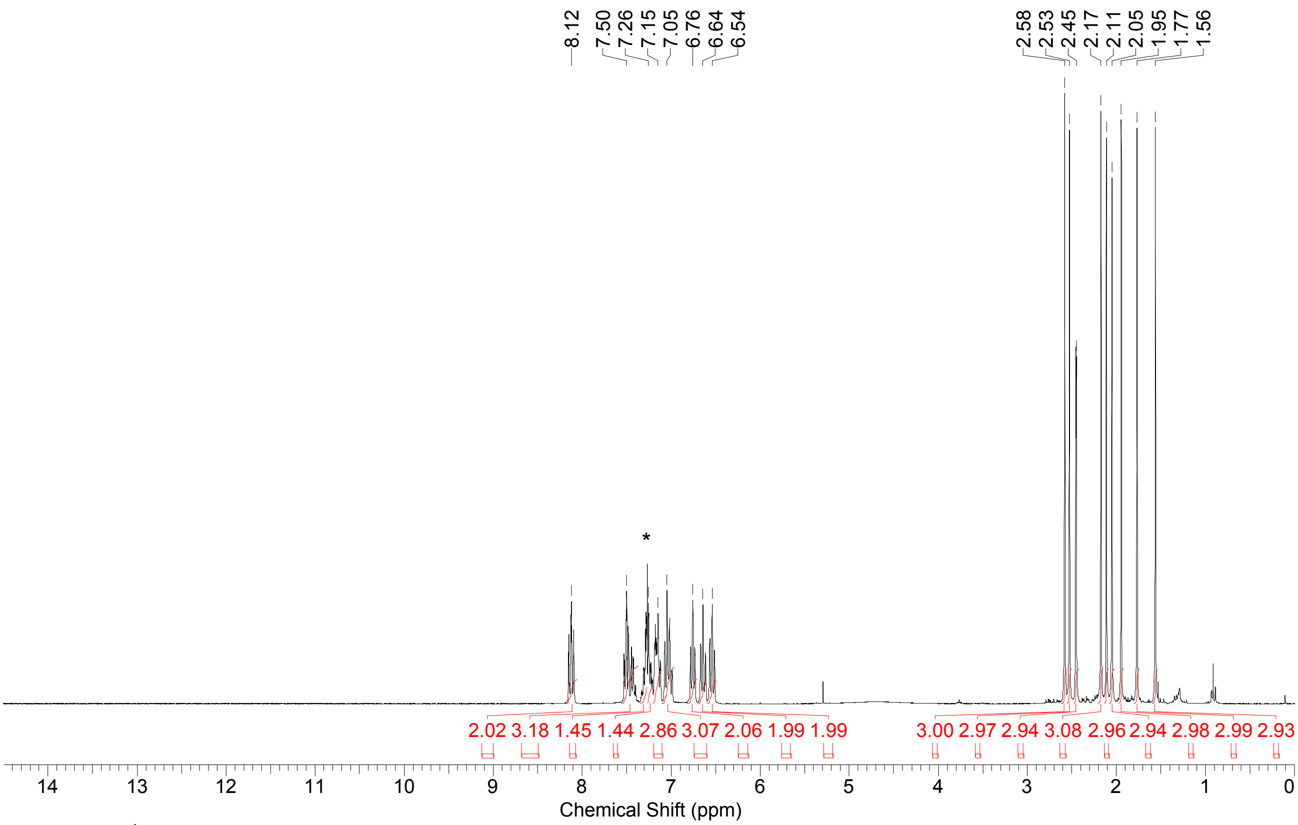

Figure S22. ^{1}H NMR of **3b** in $CDCl_3$ (*).

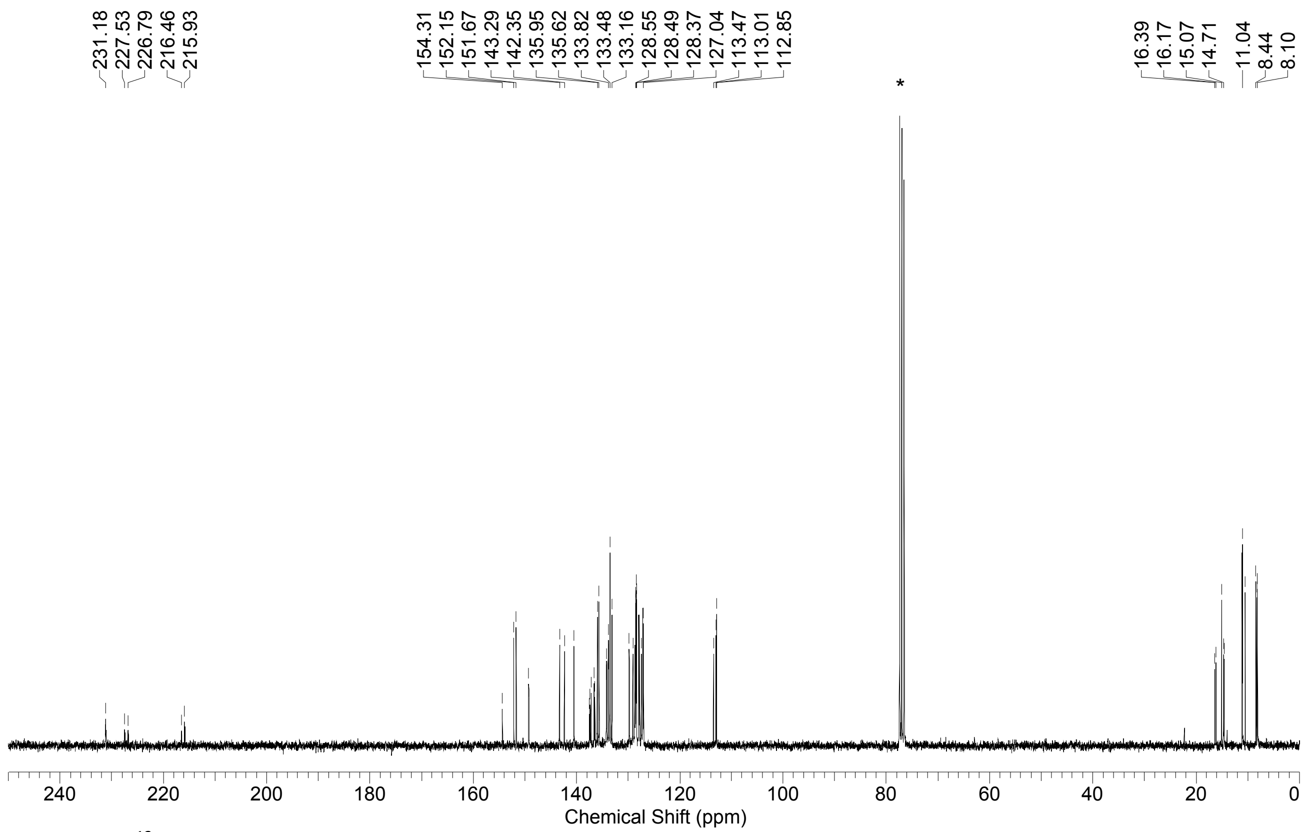

Figure S23. ^{13}C NMR of **3b** in $CDCl_3$ (*).

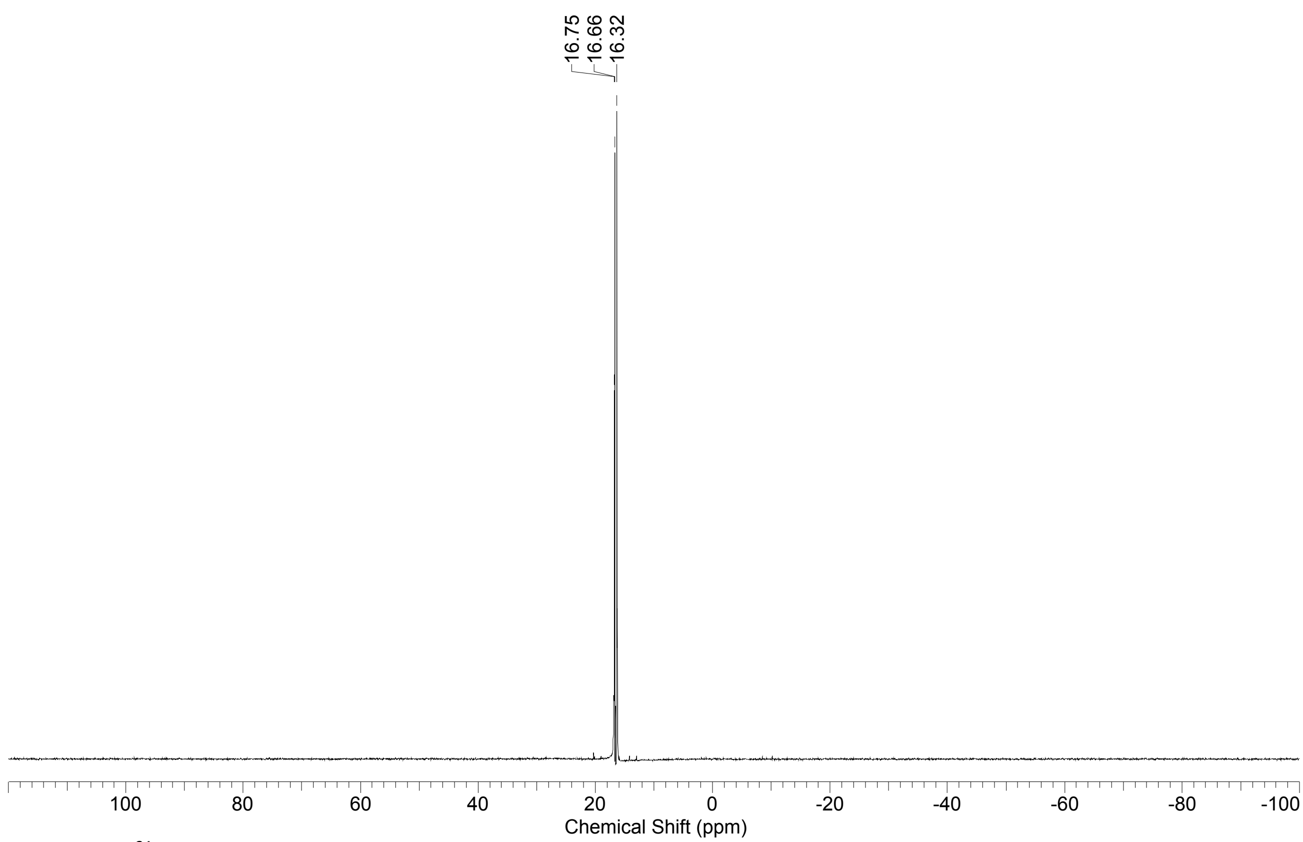

Figure S24. ^{31}P NMR of **3b** in $CDCl_3$ (*)

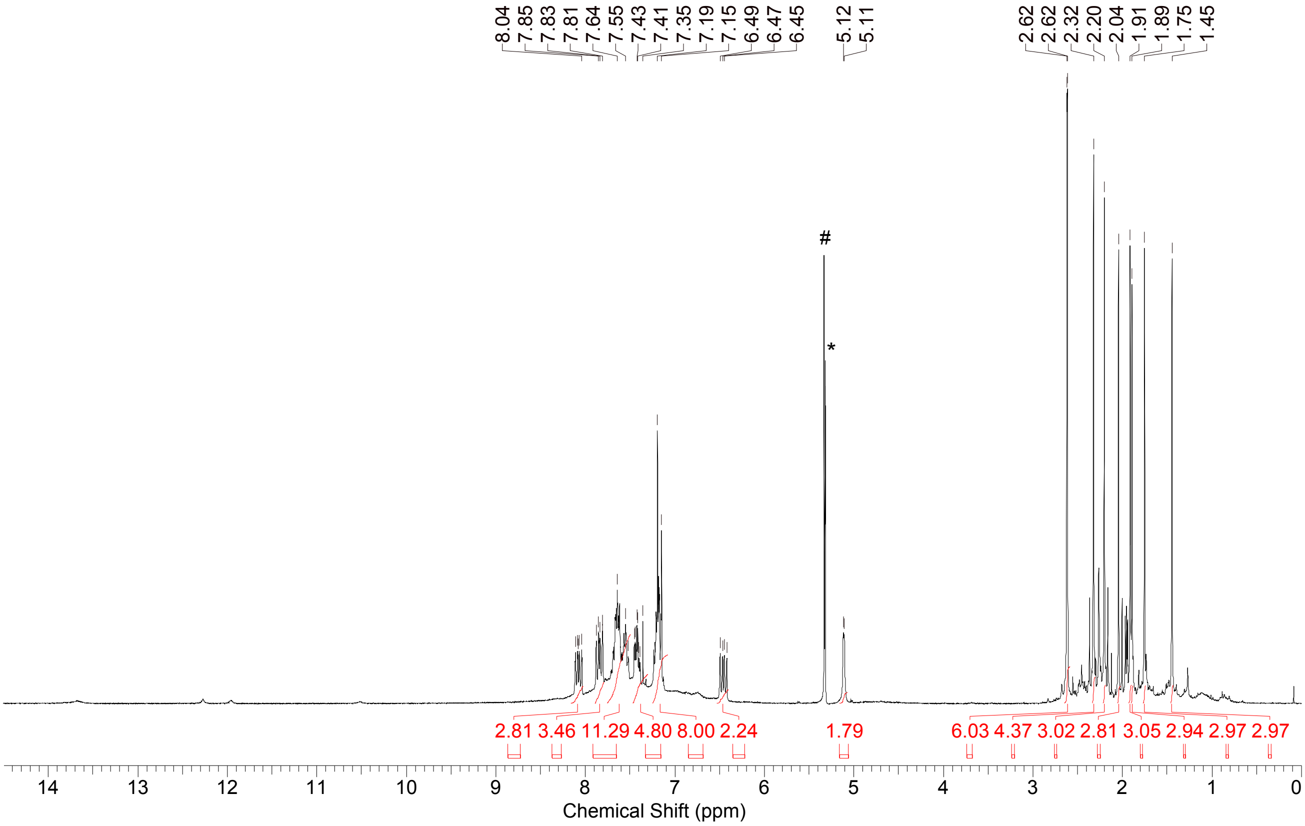

Figure S25. ^{1}H NMR of **4a**-BF_4 in CD_2Cl_2 (*). # residual CH_2Cl_2

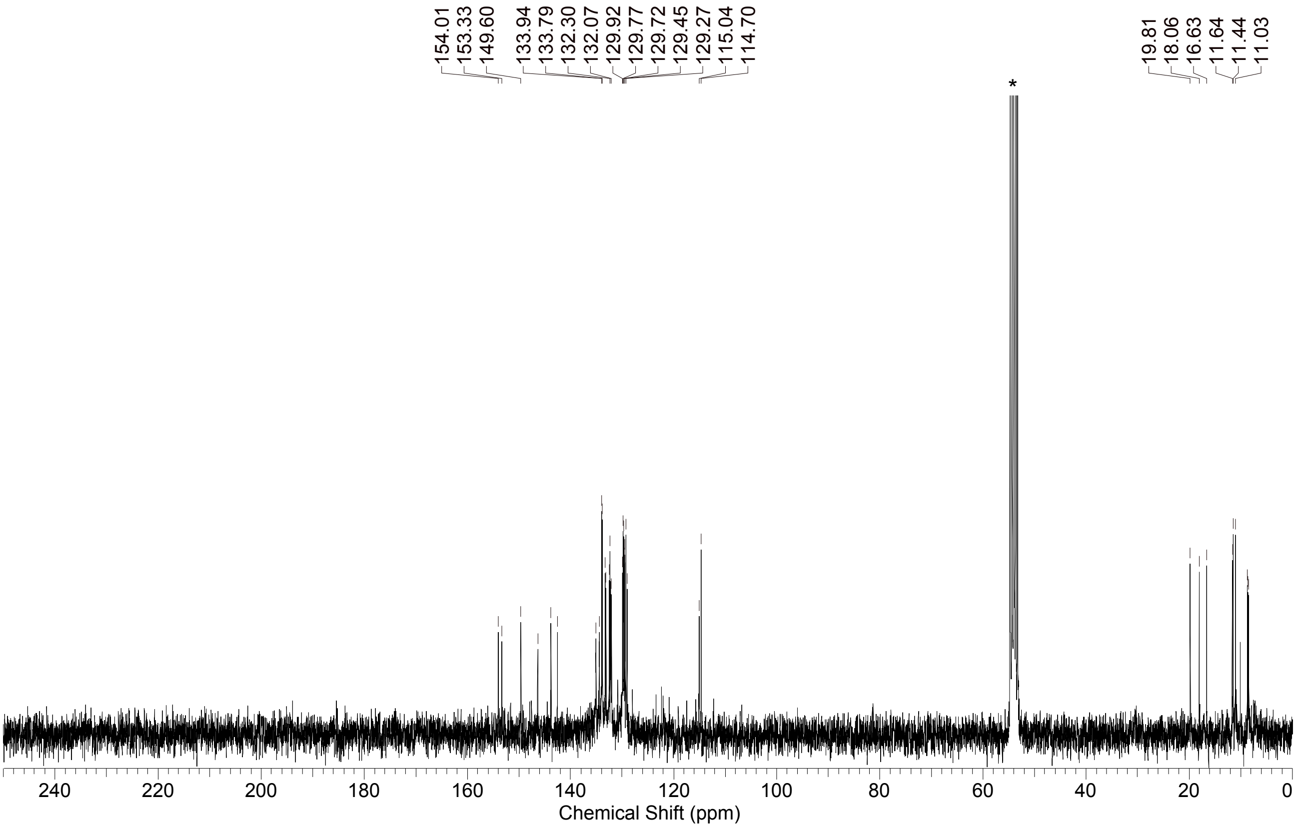

Figure S26. ^{13}C NMR of **4a**-BF_4 in CD_2Cl_2 (*).

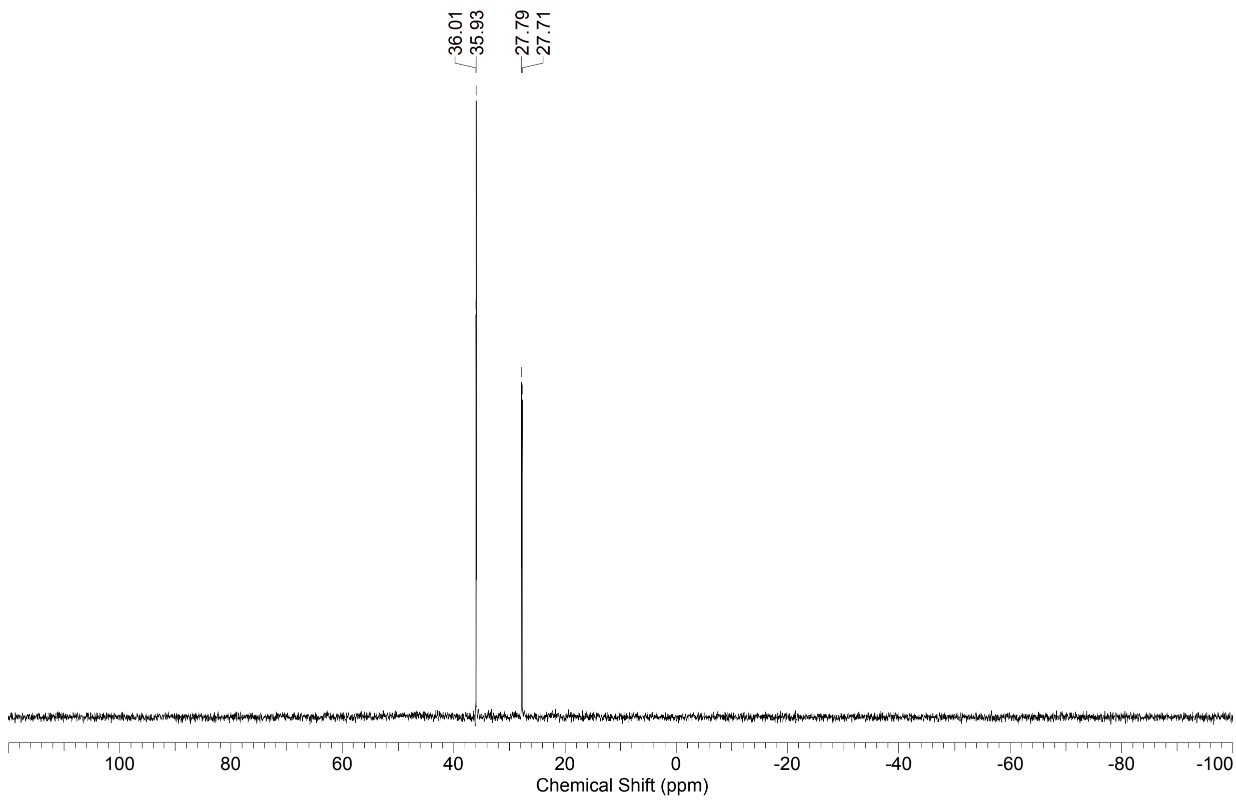

Figure S27. ^{31}P NMR of **4a**-BF_4 in CD_2Cl_2.

2.4 EPR spectra of 3a-BF_4 in frozen solution

EPR spectra in X-band were recorded by a Bruker EMX CW-micro spectrometer equipped with an ER 4131VT Digital Temperature Control System and an ER 4119HS-WI high-sensitivity optical resonator. A solution of the complex **3**-PF_6 in either CH_2Cl_2 or a CH_2Cl_2/THF mixture was filled into a J. Young EPR tube in a glovebox and introduced into the EPR spectrometer. The calibration of the *g* values was performed using DPPH (2,2-diphenyl-1-picrylhydrazyl) (g = 2.0036±0.00004). Analysis of the Spin Hamiltonian parameters was performed using the simulation program W95EPR written by F. Neese.

EPR spectra in solution were measured in CH_2Cl_2 because the reactions with NO were performed in this solvent. However, the spectrum in frozen CH_2Cl_2 solution suffers from severe line-broadening due to the poor glass forming properties of CH_2Cl_2. Spectra with a better resolution were obtained in a CH_2Cl_2/THF mixture at 100 K. While the overall metal based spin density is apparent from the g-value anisotropy (1.93, 2.04, 2.075) a stringent simulation turned out to be difficult due to at least six superimposed hfc parameters. The spectrum depicted in Figure S28 resembles the spectrum of a related 2-butine complex [Tp'WI(CO)(C_2Me_2)]BF_4, published by N. G. Connelly and co-workers,[10] which support the conclusion of a negligible dipolar hfc contribution by the P atoms.

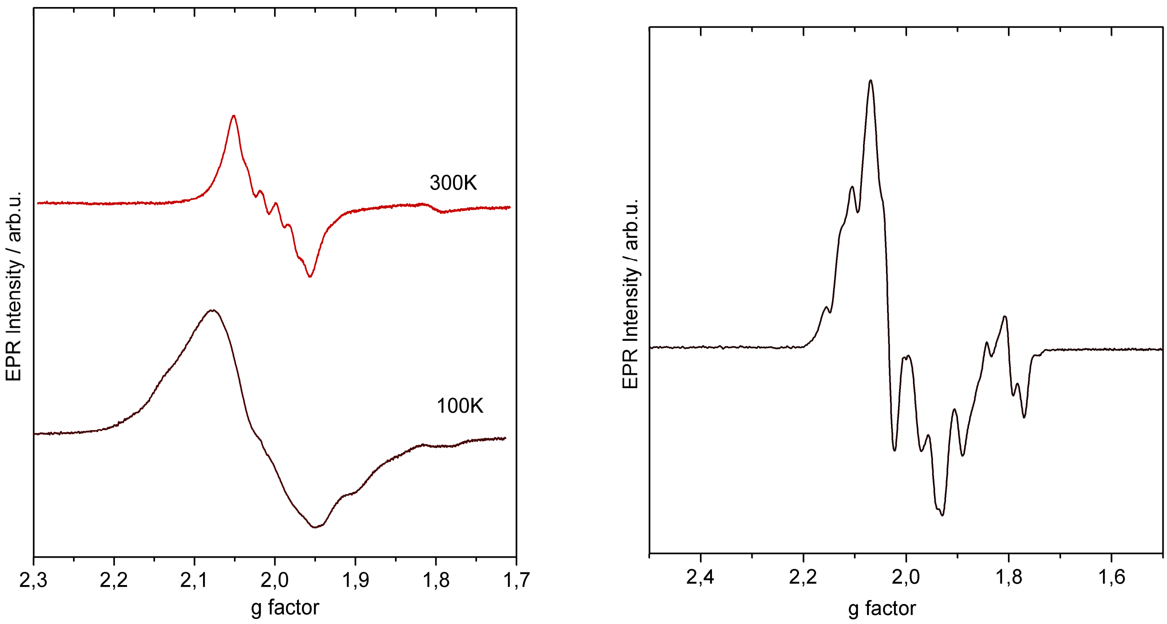

Figure S28. EPR spcetra of **3a**-BF_4 in CH_2Cl_2 (left) and in a CH_2Cl_2/THF mixture at 100 K (right).

2.5 Reactions of [NO][BF_4] with phosphines

[NO][BF_4] and the respective phosphine (one equivalent of diphosphine or two equivalents of PPh_3 for comparability of conditions) were mixed in a Schlenk flask as solids. After addition of CH_2Cl_2 the solution was stirred until all [NO][BF_4] was consumed and ^{31}P NMR indicated the end of the reaction. The solvent was removed *in vacuo* and the crude red product was analysed by means of ESI-TOF, ^{31}P NMR and ^{19}F NMR matching literature values for $Ph_3PO{\rightarrow}BF_3$,[S9] Ph_3PF_2,[S10] $[(Ph_3P)_2N]^+$,[S11] $[Ph_3PNH_2]^+$,[S12] $[Ph_3PF]^+$ [S13] and $[(Ph_2PC_2H_4PPh_2)N]^+$ [S14] (See Figures S28-S33 for the NMR spectra of the original product mixture). Single crystals suitable for XRD analysis of [($Ph_2PC_2H_4PPh_2$)N][BF_4] could be obtained after repeated slow diffusion of diethyl ether or *n*-pentane into a concentrated solution of its crude reaction mixture in CH_2Cl_2. The molecular structure is depicted in Figure S8.

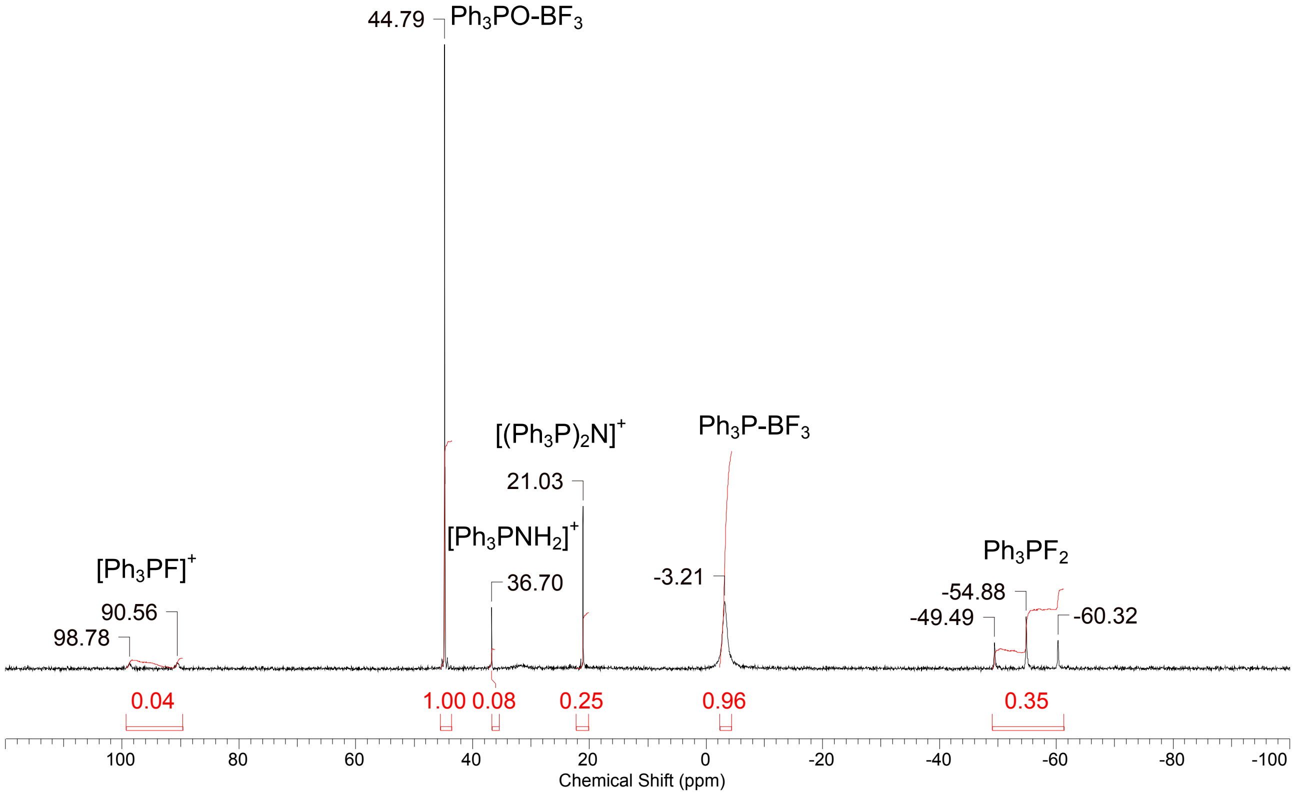

Figure S29. $^{31}P\{H\}$ NMR of the reaction mixture involving [NO][BF$_4$] and 2 PPh$_3$.

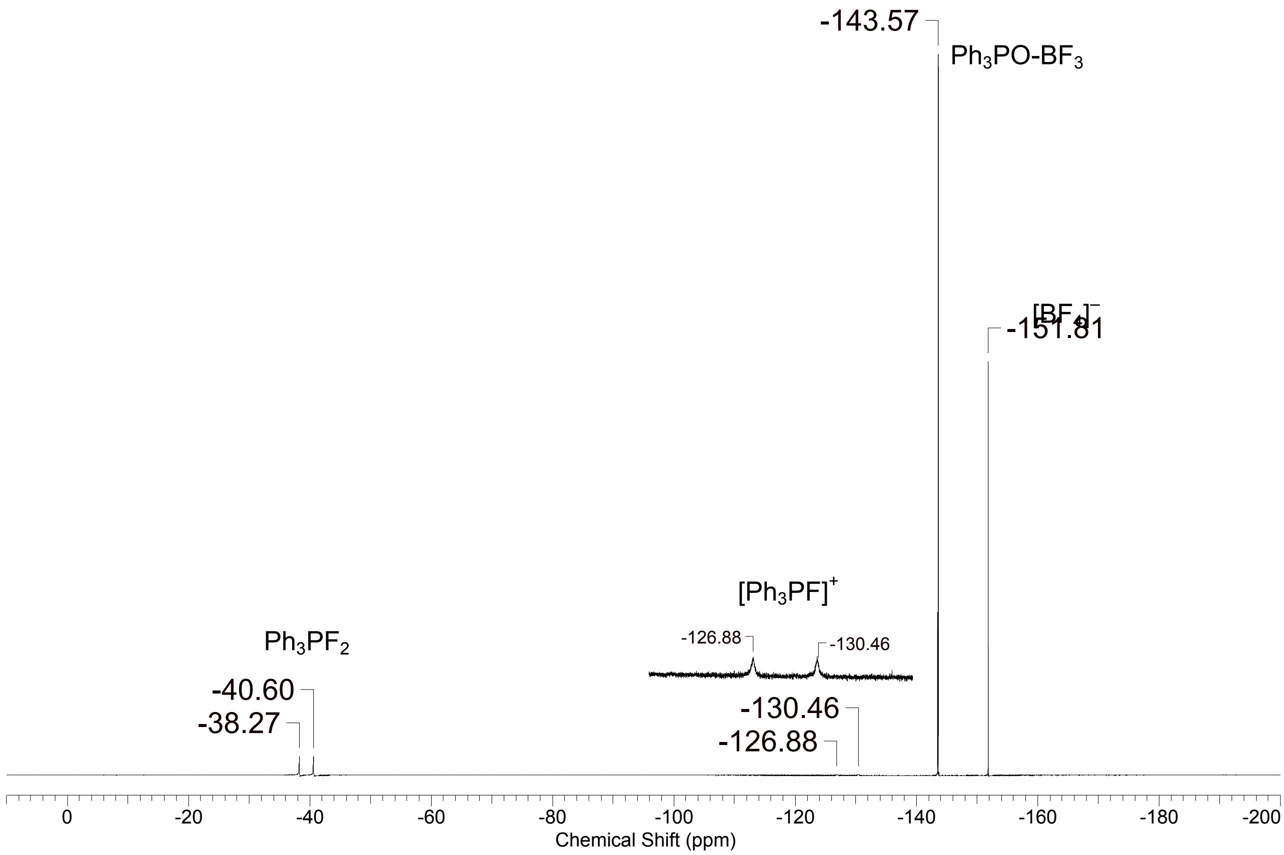

Figure S30. ^{19}F NMR of the reaction mixture involving [NO][BF$_4$] and 2 PPh$_3$.

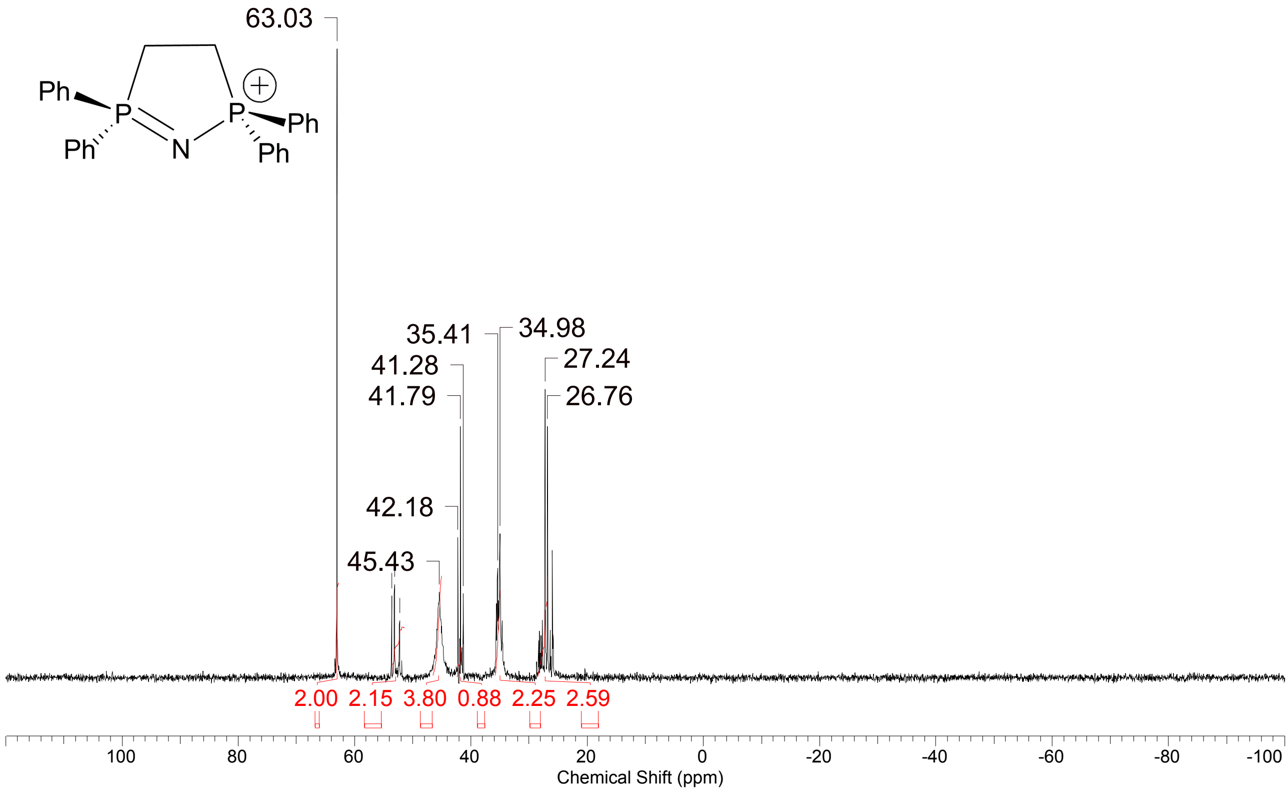

Figure S31. $^{31}P\{H\}$ NMR of the reaction mixture involving [NO][BF_4] and $Ph_2PC_2H_4PPh_2$.

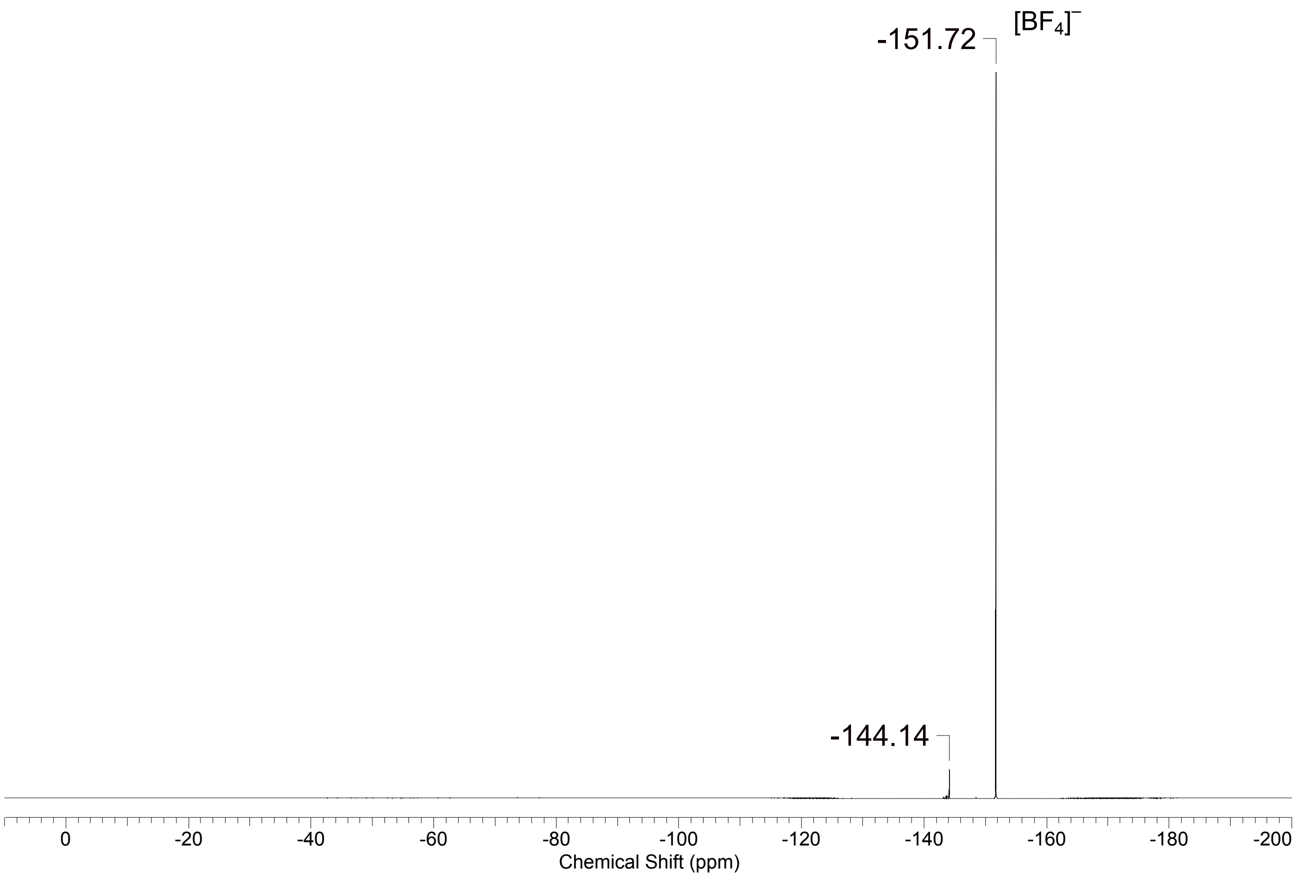

Figure S32. ^{19}F NMR of the reaction mixture involving [NO][BF_4] and $Ph_2PC_2H_4PPh_2$.

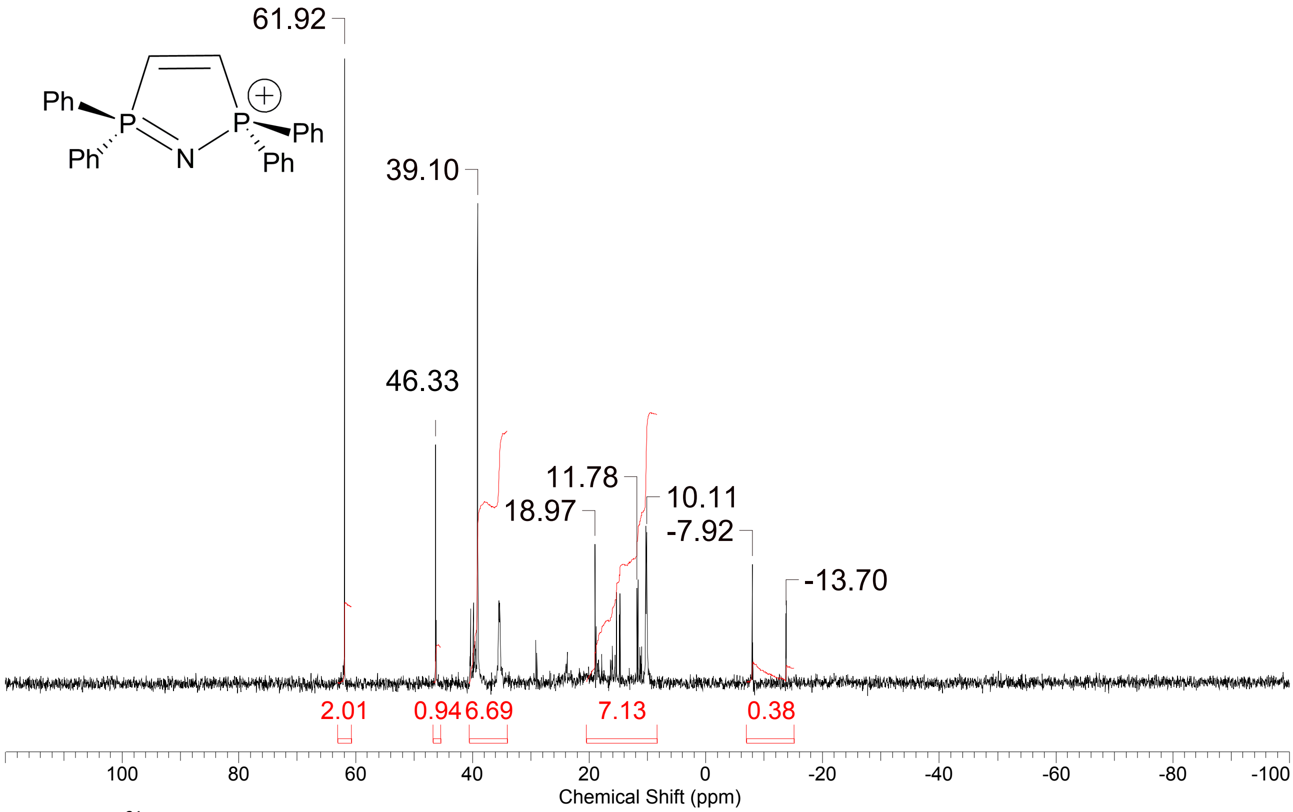

Figure S33. $^{31}P\{H\}$ NMR of the reaction mixture involving $[NO][BF_4]$ and $Ph_2PC_2H_2PPh_2$.

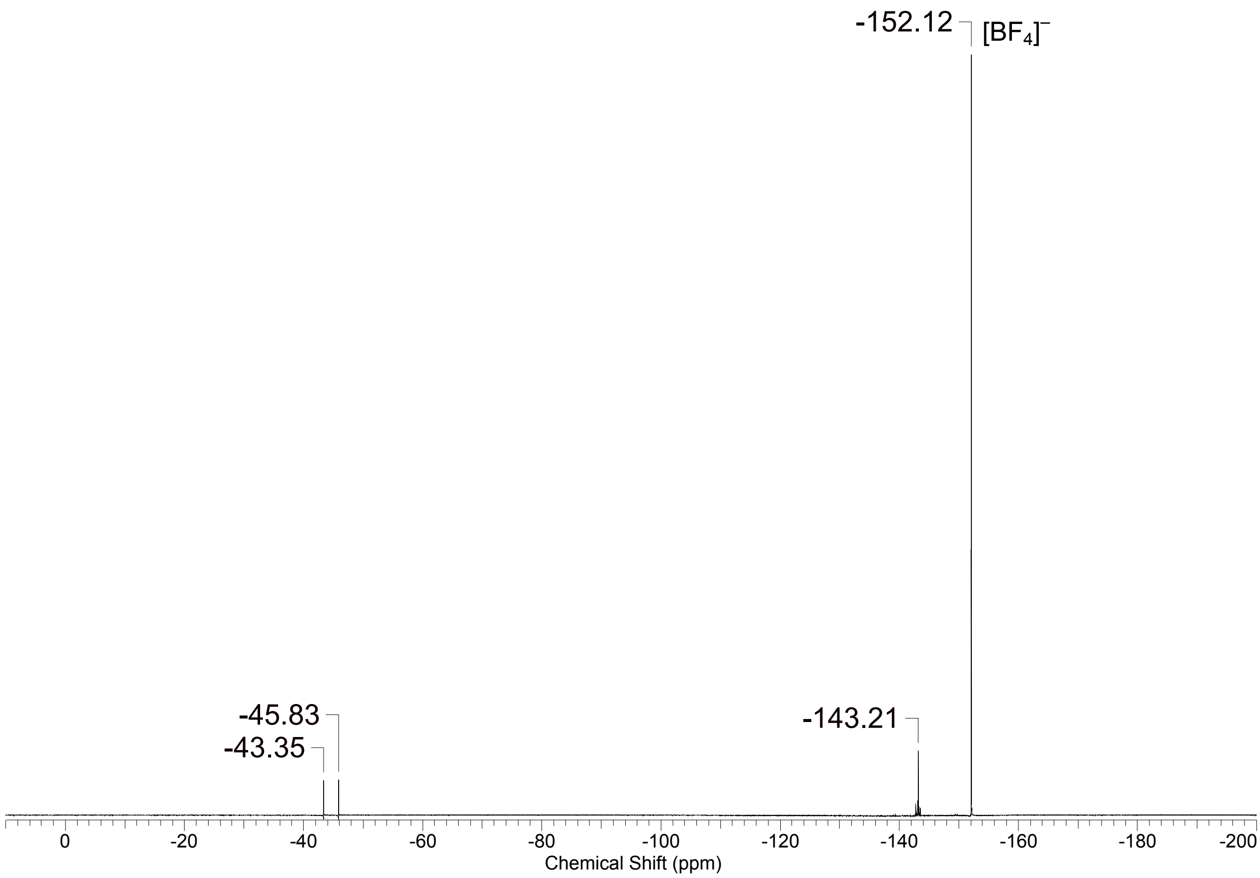

Figure S34. ^{19}F NMR of the reaction mixture involving $[NO][BF_4]$ and $Ph_2PC_2H_2PPh_2$.

2.6 Source of H-atoms for the formation of 4a-BF_4

The presented DFT calculation of H-atom transfer from the solvent solely exhibits the thermodynamic feasibility. The direct proof of such HAT steps turned out to be very challenging. Taking the $HCl_2C–H$ bond dissociation enthalpy of slightly less than 100 kcal/mol[S15] into account alternative sources come definitely in consideration (e.g. amylene stabilisers, the methyl groups of the Tp* ligand). We thoroughly conducted several labelling experiments to address the issue of the H-atom source. A simple change of the solvent from CH_2Cl_2 to CD_2Cl_2 (delivered by euriso-top®, 99.88 % atom D, no stabiliser, H_2O content < 100 ppm, which was further reduced by stirring over CaH_2 and subsequent distillation) did not lead to the expected deuterated product $[D]_2$-**4a**-BF_4 according to ESI-MS and ^1H NMR spectroscopy. However, addition of a small amount of D_2O to the product **4a**-BF_4 and immediate recording of a ^1H NMR spectrum revealed the disappearance of the NH_2 resonance. Hence, the lack of a ND_2 group could be attributed to a fast exchange with adventitious H_2O in solution.

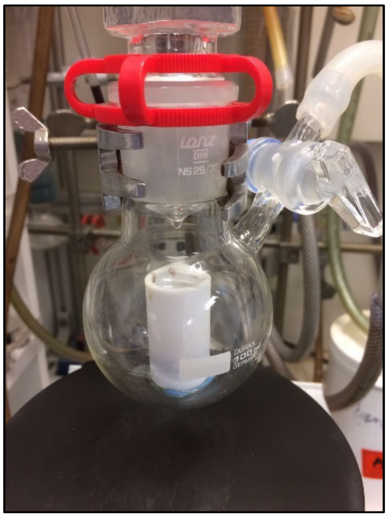

Consequently, we tried to work under strict H_2O-free conditions avoiding alternative H-atom sources. The reaction starting with **3a** and [NO][BF_4] was performed in a PTFE reaction vessel in order to circumvent glass wall contact and any H atoms coming from residues of the oxidising agent (like acetylferrocene). The reaction vessel was fixed inside a conventional Schlenk flask to ensure inert-conditions (see Figure on the right). Crystalline **3a** was carefully dried *in vacuo* for 24 h to remove any co-crystallized *n*-pentane and any traces of CH_2Cl_2 as checked by ^1H NMR. [NO][BF_4] was purified by sublimation under reduced pressure. Both reagents were placed inside the PTFE vessel and CD_2Cl_2 (which is free of the stabilisers cyclohexene or amylene) was added. When IR spectroscopy indicated the end of the reaction (≈ 45 min), the reaction mixture was transferred into a new NMR tube and directly measured. Despite all these precautions, we repeatedly detected the presence of the characteristic NH_2 signal by ^1H NMR and therefore failed to obtain the full deuterated product $[D_2]$-**4a**-BF_4. Consistently, high resolution mass spectrometry revealed the presence of a single cationic species with a typical isotope pattern for **4a**$^+$ centred at 1104.21405 m/z (calc. 1104.21483 m/z).

Generally, an intermolecular HAT mechanism was ruled out, because neither ESI-MS nor NMR spectroscopy indicated the presence of suspicious side-products and two H atoms are needed for the formation of one species **3a**$^+$. In particular, the reaction of **3a**$^+$ (purified by crystallization) and neutral NO is nearly quantitative according to ^1H and ^{31}P NMR spectra of the crude product in solution (Figure S35). Taking this observation and the isolated yields seriously, solely multiple HAT steps from sacrificial complex species with extensive degradation and final (non-apparent) precipitation has to be considered. This scenario would explain the lack of deuterated species, indeed, but remains speculation. Interestingly, the calculated *BDE* of 93.2 kcal/mol for

3a$^+$ is somewhat smaller than 99.6 kcal/mol for CH_2Cl_2 (*vide infra,* scheme S2), but this limited difference does not consequently exclude one of both options, because kinetic control might be determining.

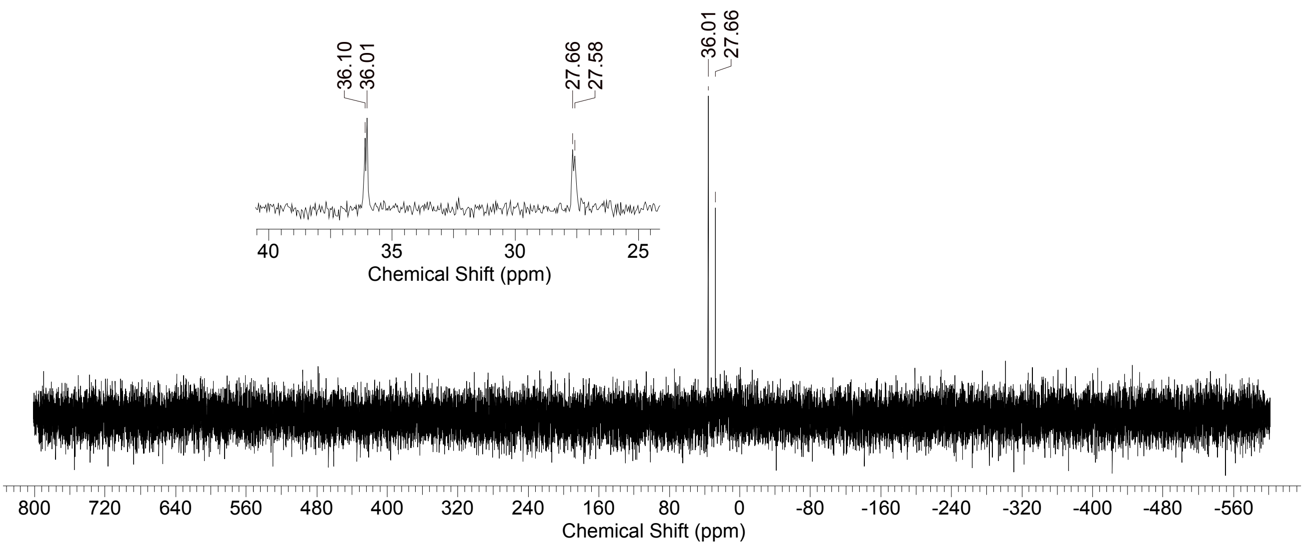

Figure S35. $^{31}P\{H\}$ NMR spectrum of the crude reaction mixture from the reaction of **3a**$^+$ with NO gas measured directly from the reaction solution.

The isolation of $[(Ph_2PC_2H_4PPh_2)N][BF_4]$ while using dppe as a diphosphine raised the idea of an alternative mechanism as shown in Scheme S1. Disproportionation of NO could lead to NO_2 and the 5-membered ring system **IM2**$^+$, which subsequently add H_2O. To prove this option pre-dried CH_2Cl_2 (CaH_2 and distillation) was saturated with $H_2{}^{18}O$ and dried again. Repeating the reaction with either neutral NO (method A) or NO^+ (method B) using this solvent with ^{18}O enriched H_2O traces did not lead to the incorporation of ^{18}O into **4a**-BF_4 as verified by high resolution ESI-MS. This observation is incompatible with the suggestion of Scheme S1.

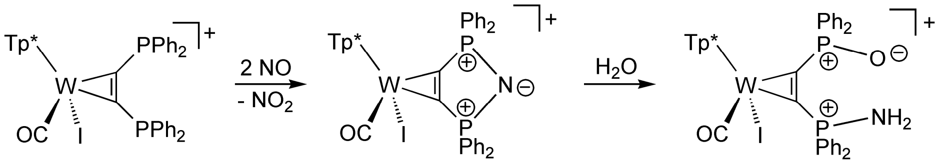

3a$^+$ **IM2**$^+$ **4a**$^+$

Scheme S1. Alternative mechanism for the formation of **4a**$^+$.

Finally, the NO gas stream could be considered as a potential source of H-atoms. However, gaseous NO is passed over drying columns filled with P_2O_5 and finally KOH. According to the supplier the NO gas contains 1000 ppm NO_2. While H_2O itself can be ruled out as an H-atom donor (*BDE* = 118.8 kcal/mol),[S16] interaction of H_2O with NO_2 could increase H-atom donor ability, but there is theoretical and spectroscopic evidence that the species $H_2O{\cdot}NO_2$ is only weakly interacting and short-lived.[S17] In addition, **4a**-BF_4 is also formed by stoichiometric use of $[NO][BF_4]$ (albeit in lower yield). Hence, the formation of the same product either from **3a**/NO^+ or **3a**$^+$/NO is likewise incompatible with such a route.

Another approach could include the determination of a kinetic isotope effect. Hence, we performed experiments with stopped-flow IR-spectroscopy. The result of the investigations with pure **3a**-BF_4 and gaseous NO in CH_2Cl_2 is shown in Figure S36. However, the deduction of a reaction order and quantitative measurements are hampered by several problems. The solubility of NO in CH_2Cl_2 is too low to attain a pseudo-first order kinetics (compare related solvents[S18]). In addition, according to DFT calculations the CO stretching frequencies of the intermediate $\mathbf{IM}^+$ and the final product $\mathbf{3a}^+$ are very close, impeding reaction tracing of the separate HAT steps by means of the strong CO resonance.

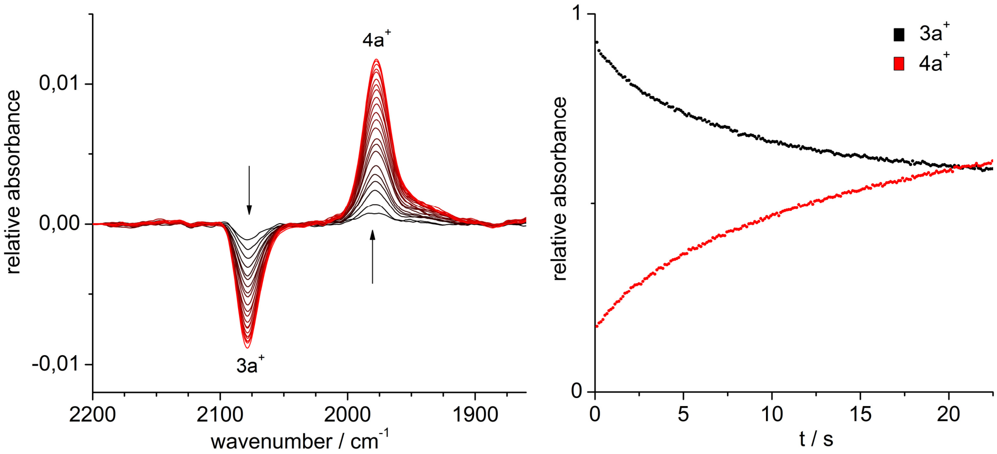

Figure S36. Stopped-flow IR measurements in CH_2Cl_2 at room temperature. Solutions of $\mathbf{3a}^+$ and NO gas in CH_2Cl_2 were mixed at room temperature and IR spectra were recorded immediately with 100 ms time resolution. The reaction started immediately without any noticeable induction period.

In the light of those exclusion experiments/arguments we consider the assumption of HAT from the solvent most likely, while any labelling studies are heavily affected by fast H/D exchange with adventitious H_2O. This applies in particular for the ESI mass spectrometry studies, which were performed by standard methods using acetonitrile. Even the NMR experiments require potentially problematic sample handling etc., which end (after H/D exchange) in comparisons of signal intensities of a broadened ^1H NMR NH_2 signal (CH_2Cl_2 vs. CD_2Cl_2). However, applying strict scientific standards, an unequivocal proof cannot be extracted from this data.

2.7 CV measurements

Cyclic voltammetry was performed on a Princeton Applied Research VersaSTAT 3 unit. A three-electrode arrangement with a glassy carbon working electrode, a platinum wire counter electrode and a Ag/$AgBF_4$ in CH_3CN reference electrode and 0.15 M *n*-Bu_4NPF_6 as supporting electrolyte was employed. The ferrocene/ferrocenium (Fc/Fc^+) redox couple was used as internal standard.

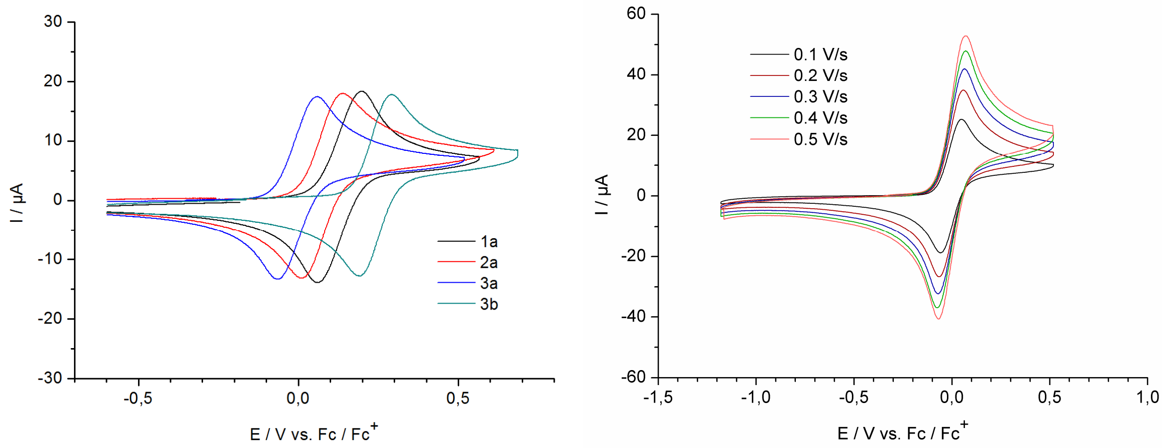

Figure S37. Cyclic voltammetry of complexes **1a**, **2a**, **3a** and **3b** measured in CH_2Cl_2; (left) comparison of the reversible oxidation waves for the putative $W^{II/III}$ redox process, v = 0.2 V/s; (right) different scan rates corroborate the reversibility of the redox process (here: **3a**).

The acetylene complex [Tp*W(CO)(I)(HC_2H)] **1a** shows a reversible oxidation at $E_{1/2}$ = +0.13 V. Stepwise substitution of H by PPh_2 leads to a more electron rich metal center as displayed by lower values for the oxidation ($E_{1/2}$ = +0.075 V for [Tp*W(CO)(I)(Ph_2PC_2H)] **2a**; $E_{1/2}$ = –0.005 V for Tp*W(CO)(I)($Ph_2PC_2PPh_2$)] **3a**). Substitution of iodide by cyanide at tungsten has a far greater impact on the oxidation potential than changes on the alkyne moiety: Complex **3b** featuring the CN^- Ligand is oxidized at $E_{1/2}$ = +0.240 V.

The compounds PPh_3, $Ph_2P(CH_2)_2PPh_2$ and cis-$Ph_2P(CH)_2Ph_2$ were measured under the same conditions exhibiting irreversible redox events in the anodic region between +0.49 to +0.80 V as compiled in Table S3. For literature values of $E_{p,a}$ for PPh_3 and other phosphines, which were obtained under different conditions, see references [S19].

Table S3. Anodic peak potentials for the oxidation of commercially available phosphines.

Compound	**$E_{p,a}$ vs. Fc/Fc^+** [mV]
PPh_3	+796
$Ph_2P(CH_2)_2PPh_2$	+486
cis-$Ph_2P(CH)_2PPh_2$	+588

3 DFT calculations

The calculations were carried out either as closed shell (S = 0) or as unrestricted open shell (S = n) calculations applying the DFT method and either the G09w[S20] or the ORCA[S21] program package. Molecular geometries were optimized without truncation and symmetry constraints in the gas phase using the BP86 functional.[S22] Pseudo-relativistic effective core potentials of the Stuttgart/Cologne group were used for W (ECP60) and I (ECP46) in combination with (8s7p6d2f1g)/[6s5p3d2f1g] basis set for W and a (4s5p)/[2s3p] basis set for I.[S23] Split valence triple ζ-basis sets (def2-TZVP) of the Ahlrich group were used for the other elements.[S24] In doing so a reasonable match between the calculated and the experimentally determined structures were achieved. A comparison of calculated and experimentally determined metric parameters for **3a**$^+$ and **4a**$^+$ are given in Table S4. Frequency calculations were performed to identify all stationary points as minima. The final energies were computed at higher level using the hybrid functional PBE0[S25] in combination with the scalar-relativistic ZORA method[S26] and the D3BJ dispersion correction of Grimme.[S27] The frontier Kohn-Sham orbitals (isosurface value 0.05) and the Mullikan spin density distribution (isosurface value 0.005) are based on the high level calculation (Fig. S38). The Gibbs free energies (ΔG) were calculated using the total electronic energy from the higher level calculation and the thermal correction to Gibbs free energy from the frequency calculation. The bond dissociation energies (*BDE*) of **3a**$^+$, [**3a**–H]$^+$, CH_2Cl_2 and $CHCl_2$ (see Scheme S2) were calculated using the BP86 functional and the def2-TZVP as above. (Preliminary examinations with a def2-SVP basis set were undertaken for all 9 different methyl groups of the Tp* ligand.) Values are given in Scheme 2 with and without zero-point correction. The standard 0.5 hartree was taken for the H atom. The total electronic energy for CH_2Cl_2 without zero point correction (as a benchmark) is in better agreement with experimental values.[S15]

Table S4. Comparison of essential bond lengths [Å] obtained by X-ray structure analysis (**3a**-PF_6, **4a**-BF_4) and single molecule geometry optimization in the gas phase (**3a**$^+$ and **4a**$^+$); the calculated bond lengths were rounded for clarity.

	3a$^+$ (calc.)	**3a**$^+$ (exp.)	**4a**$^+$ (calc.)	**4a**$^+$ (exp.)
W1–C1 (alkyne)	2.059	2.055(5)	2.054	2.036(5)
W1–C2 (alkyne)	2.082	2.062(5)	2.085	2.047(5)
C1–C2	1.340	1.345(7)	1.342	1.322(7)
W1–C3 (CO)	2.046	2.090(5)	1.982	1.985(6)
W1–N1 (Tp*)	2.231	2.234(4)	2.221	2.210(4)
W1–N3 (Tp*)	2.164	2.138(4)	2.191	2.186(4)
W1–N5 (Tp*)	2.203	2.178(4)	2.250	2.248(4)
W1–I1	2.722	2.7276(4)	2.754	2.7739(4)
C1–P1	1.768	1.766(5)	1.752	1.770(5)
C2–P2	1.782	1.779(5)	1.822	1.826(5)
P1–N7	–	–	1.659	1.609(5)
P2–O2	–	–	1.516	1.487(4)

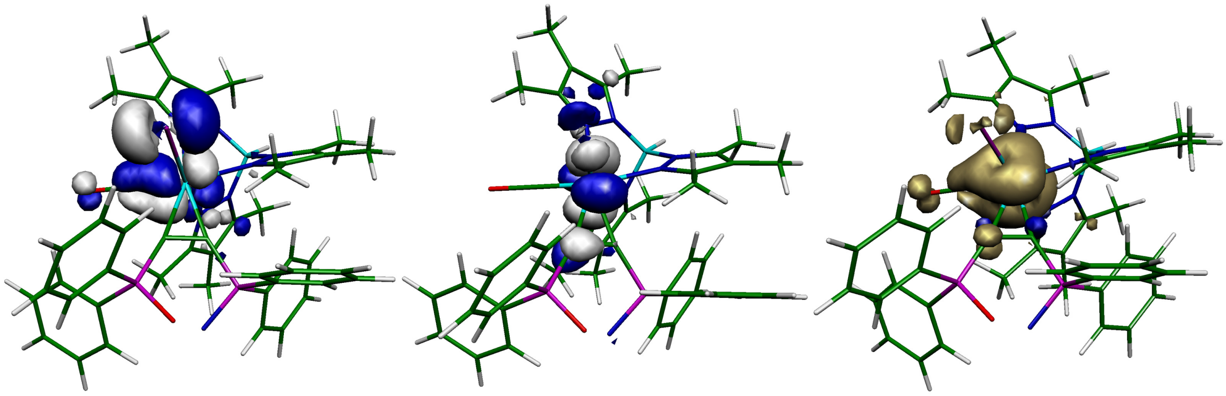

Figure S38. Magnetic orbitals 271a (left) and 272a (middle) and resulting spin density distribution (right) for the triplet state ^{3}**IM**$^+$ of the intermediate **IM**$^+$ after NO addition.

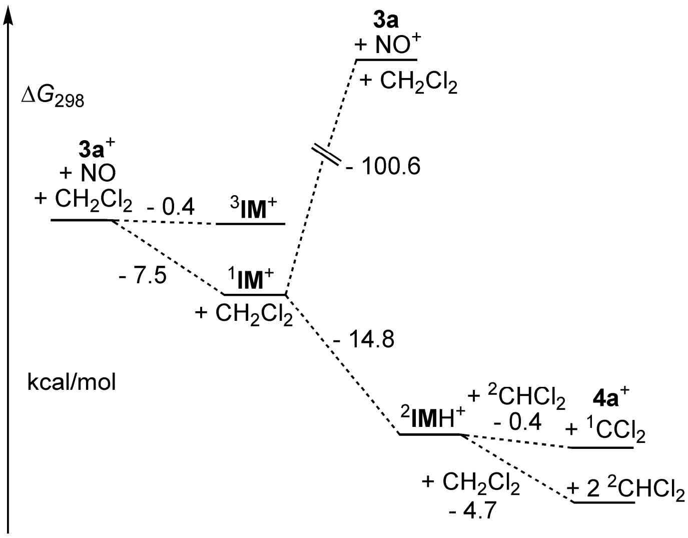

Figure S39. Calculated Gibbs energy profile of the reaction **3a**$^+$ with NO and alternatively **3a** with NO$^+$ to **4a**$^+$ based on two subsequent single H atom transfer steps. (The strong bias **3a**/NO$^+$ to **3a**$^+$/NO reflects the potential difference $E°(NO/NO^+)$ = 1.0 V and $E°$ (**3a**/**3a**$^+$) = –0.005 V. In addition, the lack of solvation in the gas phase calculation is more drastic for the small NO$^+$ compared with **3a**$^+$.)

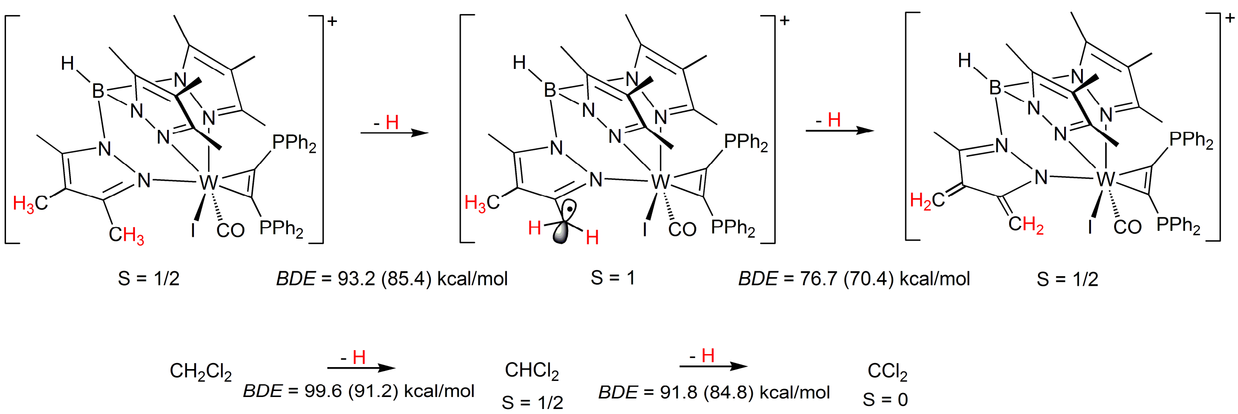

Scheme S2. Calculated bond dissociation energies (*BDE*) in comparison; without and with zero point correction (values in brackets).

Table S5. Cartesian coordinates of the geometry optimized structures of **3a**$^{+}$ (left) and ^{1}**IM**$^{+}$ (right) in the gas phase; PB86/def2-TZVP/ECP(W, I).

W	0.521936	-0.671841	-0.001623	I	0.449738	-1.703694	-2.804440
I	-0.067778	-2.249925	-2.210468	W	0.625286	-0.703691	-0.161847
C	-0.107174	-2.137657	1.282532	C	0.739691	1.841518	-3.038362
C	-1.512809	-0.296747	0.313125	C	1.849391	-4.328213	-0.594334
C	-0.906694	0.833544	-0.109966	N	2.016610	0.845294	-1.084249
N	2.439901	-1.877947	0.169893	N	2.521394	-1.932224	-0.049202
N	1.755931	0.619603	-1.318415	N	1.455170	-0.046828	1.760730
N	1.456219	0.320146	1.698992	C	-0.185962	-2.361960	0.579937
H	-0.528153	0.748449	-2.824495	C	-0.824174	0.783560	-0.177285
O	-0.383177	-2.924926	2.076385	C	-1.388080	-0.398093	0.184606
P	-3.141423	-0.713519	0.940075	C	1.935965	1.663888	-2.168084
P	-1.461884	2.419830	-0.691792	C	2.813505	-3.257524	-0.207220
C	2.758276	-3.206299	0.215946	N	3.281716	1.004640	-0.572435
N	3.628325	-1.188548	0.256833	N	3.695071	-1.311948	0.317934
C	1.567844	1.218122	-2.527694	N	2.740733	0.440433	1.824469
N	3.025399	0.958332	-0.904687	C	0.929224	0.065837	3.012032
N	2.767995	0.723539	1.612289	O	-0.679759	-3.321033	1.023580
C	1.012044	0.657754	2.949201	P	-1.768923	2.300533	0.082358
C	0.343945	1.112999	-3.373656	P	-3.132303	-0.596112	0.568625
C	-3.338392	-2.540027	0.988960	C	3.157969	2.344438	-2.346865
C	-4.272488	-0.206829	-0.416283	C	4.179252	-3.473529	0.050001
C	-2.678994	3.039582	0.546980	C	3.989332	1.895900	-1.318201
C	-0.082375	3.622176	-0.558402	B	3.722793	0.195937	0.652575
C	1.793510	-4.345161	0.197550	C	4.703513	-2.219531	0.381606
C	4.154045	-3.355368	0.309031	C	3.018000	0.850938	3.090322
C	4.670980	-2.055250	0.336820	C	-0.455119	-0.336671	3.374841
B	3.625608	0.349182	0.371505	C	1.877744	0.644092	3.874711
C	2.723435	1.936028	-2.886808	C	-0.826187	3.529766	1.001483
C	3.624508	1.749652	-1.834202	C	-2.265200	2.969133	-1.530326
C	3.145237	1.310549	2.775532	C	-3.545756	-1.132365	2.239641
C	2.047847	1.293165	3.652919	C	-3.945082	-1.691467	-0.593424
C	-0.353407	0.353966	3.465323	C	3.467594	3.320907	-3.439380
H	0.517317	0.430125	-4.221297	C	4.894000	-4.787635	-0.025786
H	0.097443	2.099459	-3.794153	C	5.408698	2.261333	-1.024214
C	-3.339985	-3.366859	-0.148411	C	6.105158	-1.853186	0.747015
C	-3.594648	-3.107041	2.249733	C	4.350165	1.395733	3.491054
C	-5.593279	0.099821	-0.042003	C	1.687005	0.950947	5.329393
C	-3.915444	-0.161728	-1.774791	C	0.542709	3.721849	0.752944
C	-3.986872	3.289115	0.100274	C	-1.495333	4.322243	1.953019
C	-2.335272	3.351610	1.874382	C	-2.754725	2.122082	-2.541313
C	-0.115139	4.686667	-1.478591	C	-2.275580	4.361998	-1.725180
C	0.919223	3.605828	0.426675	C	-4.057584	-0.207736	3.168462

H	1.621568	-4.729960	1.216012	C	-3.441593	-2.495328	2.573830
H	2.213870	-5.173628	-0.390709	C	-5.305826	-1.987418	-0.371085
H	0.825533	-4.084362	-0.240121	C	-3.286357	-2.185739	-1.731514
C	4.901465	-4.651773	0.367557	C	1.236685	4.710785	1.454054
C	6.093378	-1.607800	0.426641	C	-0.787069	5.301818	2.651755
H	4.743685	0.749756	0.529398	C	-3.249748	2.665348	-3.727702
C	2.915438	2.718260	-4.148491	C	-2.766863	4.896773	-2.917866
C	5.011350	2.281827	-1.679722	C	-4.455405	-0.655239	4.429750
C	4.520098	1.842509	3.012641	C	-3.834672	-2.924865	3.842433
C	1.998348	1.811380	5.057824	C	-5.997187	-2.771147	-1.293140
H	-1.141637	0.543056	2.726331	C	-3.989243	-2.979411	-2.640473
H	-0.560681	0.971529	4.348745	C	0.575020	5.498587	2.401295
H	-0.438488	-0.697834	3.781496	C	-3.256335	4.051033	-3.917826
H	-3.173835	-2.938979	-1.137926	C	-4.339987	-2.007247	4.769357
C	-3.568469	-4.738113	-0.017716	C	-5.339652	-3.268843	-2.424868
C	-3.827530	-4.479386	2.376669	H	0.947847	1.484021	-4.058480
H	-3.615211	-2.466647	3.134789	H	1.006035	-3.944919	-1.178398
H	-5.877028	0.081409	1.012693	H	0.477588	2.909058	-3.113267
C	-6.542709	0.430440	-1.011223	H	-0.129952	1.294640	-2.667142
C	-4.864961	0.187994	-2.739545	H	2.368163	-5.080277	-1.205823
H	-2.899578	-0.415227	-2.083646	H	1.452392	-4.847908	0.292210
H	-4.259411	3.057340	-0.931202	H	4.829645	0.519244	0.979793
C	-4.937846	3.833775	0.969089	H	-0.550146	-0.398508	4.466745
C	-3.289036	3.887973	2.740570	H	-1.198642	0.394806	3.020195
H	-1.314243	3.196612	2.227752	H	-0.717343	-1.315376	2.954037
H	-0.890626	4.712295	-2.248375	H	2.703606	4.111316	-3.505649
C	0.826032	5.717082	-1.409695	H	4.436245	3.813366	-3.280259
C	1.863190	4.634001	0.488076	H	3.507423	2.829404	-4.424818
H	0.957581	2.792908	1.152000	H	4.817987	-5.233846	-1.030023
H	4.663018	-5.295355	-0.493642	H	5.962420	-4.678829	0.202250
H	4.657381	-5.223287	1.276879	H	4.479365	-5.518440	0.685959
H	5.987486	-4.491305	0.363826	H	5.743512	3.041146	-1.719625
H	6.368895	-0.956493	-0.415157	H	5.536461	2.643450	-0.001165
H	6.760541	-2.478158	0.411445	H	6.084476	1.400839	-1.140945
H	6.290916	-1.050125	1.354090	H	6.754137	-2.733559	0.663547
H	3.876092	3.249632	-4.152661	H	6.509289	-1.072492	0.086989
H	2.123175	3.471734	-4.280251	H	6.175906	-1.481303	1.779970
H	2.895555	2.067801	-5.037226	H	4.291378	1.822189	4.500262
H	5.131052	2.847211	-0.744638	H	5.123719	0.612868	3.505021
H	5.245875	2.955901	-2.512623	H	4.693293	2.184334	2.807305
H	5.762060	1.477490	-1.680148	H	1.546665	0.035038	5.925213
H	5.238755	1.028906	3.198064	H	2.557979	1.475052	5.744547
H	4.523940	2.492385	3.896704	H	0.808118	1.591148	5.499609
H	4.891253	2.420035	2.156054	H	1.062699	3.101828	0.020318
H	2.776161	2.566679	5.234154	H	-2.558894	4.165810	2.137027
H	2.149942	1.007777	5.796118	H	-2.747266	1.038918	-2.411637

H	1.030285	2.281579	5.282701	H	-1.899579	5.028519	-0.947344
H	-3.566892	-5.373523	-0.905473	H	-4.133294	0.845953	2.898061
C	-3.810899	-5.295976	1.243154	H	-3.064093	-3.219663	1.851299
H	-4.028444	-4.908181	3.360125	H	-5.818818	-1.606789	0.513901
H	-7.567522	0.656028	-0.710430	H	-2.229693	-1.969405	-1.910282
C	-6.178962	0.480311	-2.360963	H	2.298611	4.866003	1.257252
H	-4.578566	0.220390	-3.792547	H	-1.303669	5.917546	3.390041
H	-5.949319	4.029902	0.608975	H	-3.628999	2.003100	-4.507717
C	-4.591619	4.130640	2.289231	H	-2.767385	5.978200	-3.064706
H	-3.013847	4.128476	3.769443	H	-4.861244	0.058114	5.149035
H	0.782277	6.540464	-2.125003	H	-3.754798	-3.981717	4.101566
C	1.818054	5.692204	-0.425449	H	-7.051253	-2.998172	-1.126227
H	2.630421	4.617011	1.264864	H	-3.473379	-3.373214	-3.517602
H	-3.997636	-6.367288	1.338633	H	1.121902	6.271279	2.944952
H	-6.920064	0.743570	-3.117881	H	-3.641381	4.471967	-4.848306
H	-5.332613	4.559594	2.966339	H	-4.653192	-2.349251	5.757501
H	2.551813	6.498282	-0.367319	H	-5.884319	-3.888990	-3.139186
				O	-3.786247	0.851039	0.293200
				N	-3.004376	1.898093	1.105549

Table S6. Cartesian coordinates of the geometry optimized structures of ^{3}**IM**$^{+}$ (left) and ^{2}**IM**-H^{+} (right) in the gas phase; PB86/def2-TZVP/ECP(W, I).

I	0.138006	-1.784035	-2.695797	I	-0.746519	-2.207576	-2.171987
W	0.721287	-0.724912	-0.154023	W	0.194969	-0.815025	0.019796
C	0.741845	1.711275	-3.094586	C	0.790145	0.757617	-3.368604
C	1.920537	-4.342434	-0.713757	C	0.031204	-4.664747	0.477907
N	2.049265	0.789503	-1.132895	N	1.877582	-0.126900	-1.259869
N	2.598990	-1.950685	-0.142323	N	1.535443	-2.603405	0.395269
N	1.512202	0.086054	1.712239	N	1.349584	-0.089214	1.697773
C	-0.017956	-2.378098	0.789788	C	-1.068873	-1.874436	1.200391
C	-0.869966	0.755279	-0.141584	C	-0.581214	1.138800	-0.128759
C	-1.445594	-0.404924	0.150698	C	-1.592711	0.310758	0.113262
C	1.947527	1.589928	-2.230478	C	1.957230	0.415958	-2.507716
C	2.889985	-3.268869	-0.342656	C	1.339963	-3.951066	0.539564
N	3.318536	0.968013	-0.634595	N	3.168506	-0.297764	-0.816644
N	3.776577	-1.342937	0.228302	N	2.887244	-2.389295	0.546845
N	2.852655	0.404885	1.781453	N	2.723747	-0.175067	1.677746
C	0.984330	0.351988	2.942407	C	1.000098	0.538477	2.863429
O	-0.416506	-3.308637	1.350316	O	-1.760715	-2.481513	1.900365
P	-1.796565	2.297393	0.068922	P	-0.476270	3.002551	-0.026640
P	-3.149530	-0.577865	0.633705	P	-3.434808	0.533187	0.120809
C	3.159772	2.277885	-2.432530	C	3.308908	0.587152	-2.861637
C	4.262076	-3.491419	-0.113286	C	2.572693	-4.586240	0.766422
C	4.005607	1.855274	-1.402072	C	4.046750	0.121277	-1.766358
B	3.798856	0.155451	0.581687	B	3.445900	-0.952384	0.550630

C	4.790892	-2.249249	0.245142	C	3.529839	-3.563759	0.767858
C	3.155661	0.869293	3.020908	C	3.231488	0.385316	2.803262
C	-0.441277	0.127582	3.303400	C	-0.400698	0.838010	3.266682
C	1.985724	0.846914	3.793442	C	2.161229	0.851368	3.585240
C	-0.824055	3.563617	0.905479	C	1.159297	3.429116	0.648318
C	-2.300480	2.890027	-1.572652	C	-0.525679	3.600997	-1.752350
C	-3.445365	-1.117019	2.332830	C	-4.011045	0.820721	1.825842
C	-4.104875	-1.649204	-0.444456	C	-4.203676	-0.982857	-0.525643
C	3.454269	3.237521	-3.544133	C	3.820679	1.136069	-4.157480
C	4.971679	-4.804520	-0.236699	C	2.787451	-6.055188	0.964406
C	5.421140	2.246503	-1.125566	C	5.529155	0.043956	-1.598284
C	6.198051	-1.887734	0.594187	C	5.007229	-3.657913	0.965611
C	4.530001	1.304088	3.412474	C	4.695810	0.450185	3.083040
C	1.817424	1.253649	5.225938	C	2.224513	1.547470	4.909394
C	0.527795	3.763508	0.581729	C	2.362969	3.022763	0.052155
C	-1.451906	4.379277	1.865249	C	1.188941	4.296899	1.753857
C	-2.749354	1.992624	-2.558208	C	-1.637732	3.277240	-2.553347
C	-2.374109	4.274752	-1.809625	C	0.441144	4.498687	-2.240820
C	-3.891106	-0.188168	3.290796	C	-4.763237	1.998653	1.985492
C	-3.302030	-2.474599	2.673418	C	-3.831906	-0.037643	2.924390
C	-5.424633	-1.960981	-0.059123	C	-4.649929	-2.050965	0.268972
C	-3.598461	-2.109557	-1.670133	C	-4.430907	-1.009904	-1.914111
C	1.245995	4.779793	1.216405	C	3.582382	3.485911	0.553637
C	-0.721011	5.388144	2.496040	C	2.411963	4.752047	2.252672
C	-3.268274	2.476874	-3.760333	C	-1.762725	3.830279	-3.829338
C	-2.887478	4.750796	-3.017461	C	0.305177	5.048972	-3.518281
C	-4.180249	-0.624241	4.585629	C	-5.326593	2.309669	3.224820
C	-3.585403	-2.894242	3.974100	C	-4.397654	0.280228	4.161246
C	-6.226937	-2.725050	-0.905113	C	-5.295148	-3.140543	-0.321447
C	-4.408680	-2.883558	-2.503420	C	-5.078427	-2.099995	-2.497119
C	0.624350	5.590931	2.170984	C	3.609709	4.351702	1.651798
C	-3.337905	3.854180	-3.991669	C	-0.792439	4.712324	-4.316496
C	-4.022380	-1.970608	4.929827	C	-5.144291	1.452903	4.313494
C	-5.719323	-3.188330	-2.124831	C	-5.506655	-3.168387	-1.703093
H	0.878825	1.157523	-4.037266	H	0.646950	-0.005113	-4.150908
H	0.981522	-3.953763	-1.117216	H	-0.718995	-4.133728	-0.115735
H	0.567049	2.765991	-3.356073	H	0.964605	1.718720	-3.874255
H	-0.156296	1.316612	-2.613346	H	-0.143406	0.836299	-2.804358
H	2.366167	-4.993079	-1.480902	H	0.177682	-5.654803	0.023201
H	1.693897	-4.981439	0.155597	H	-0.379076	-4.831900	1.486879
H	4.911672	0.487928	0.877886	H	4.624741	-0.969457	0.764158
H	-0.559218	0.182014	4.393272	H	-0.421441	1.135825	4.322704
H	-1.108176	0.883337	2.858967	H	-0.837150	1.668159	2.683203
H	-0.795671	-0.860172	2.980084	H	-1.058493	-0.033061	3.154020
H	2.674628	4.010359	-3.629866	H	3.289877	2.057406	-4.440849
H	4.411538	3.753253	-3.390498	H	4.890833	1.375966	-4.100985

H	3.509560	2.726867	-4.518838	H	3.688466	0.419834	-4.984144
H	4.870410	-5.227140	-1.248940	H	2.407307	-6.639277	0.111651
H	6.045522	-4.703666	-0.031380	H	3.852945	-6.294782	1.074860
H	4.571991	-5.551914	0.466833	H	2.273165	-6.423659	1.865644
H	5.739395	3.019545	-1.835956	H	6.025986	0.602305	-2.401482
H	5.549354	2.646479	-0.109586	H	5.858751	0.459926	-0.636481
H	6.107772	1.393478	-1.232545	H	5.887708	-0.995766	-1.648654
H	6.843981	-2.768996	0.496536	H	5.314120	-4.710476	0.995137
H	6.596522	-1.104551	-0.066931	H	5.560415	-3.166670	0.153140
H	6.284816	-1.522252	1.628267	H	5.323207	-3.190864	1.910639
H	4.519652	1.701015	4.434997	H	4.874552	0.986294	4.022660
H	5.246849	0.469987	3.383500	H	5.138963	-0.552371	3.174412
H	4.915378	2.090531	2.747921	H	5.234981	0.979267	2.284224
H	1.450562	0.419358	5.844263	H	1.557930	1.074073	5.646042
H	2.768392	1.585135	5.663041	H	3.239137	1.524737	5.327788
H	1.100861	2.082256	5.334791	H	1.924706	2.603475	4.825055
H	1.017082	3.129292	-0.159862	H	2.352945	2.363195	-0.816491
H	-2.502918	4.217662	2.108062	H	0.241767	4.615679	2.191521
H	-2.685506	0.915212	-2.397097	H	-2.417212	2.617276	-2.163591
H	-2.030711	4.980811	-1.051684	H	1.294208	4.781329	-1.623140
H	-4.002599	0.861483	3.016183	H	-4.910676	2.655406	1.126557
H	-2.984051	-3.205664	1.928619	H	-3.256749	-0.957918	2.831199
H	-5.821077	-1.607972	0.894411	H	-4.526451	-2.029682	1.351448
H	-2.572657	-1.879476	-1.968416	H	-4.123920	-0.159307	-2.524002
H	2.295043	4.938743	0.961611	H	4.514200	3.183665	0.071744
H	-1.207380	6.022059	3.239474	H	2.427205	5.437640	3.102145
H	-3.616039	1.774834	-4.520015	H	-2.630816	3.578982	-4.441778
H	-2.936821	5.826248	-3.196689	H	1.056270	5.750964	-3.885612
H	-4.535210	0.093180	5.327521	H	-5.911210	3.224302	3.336968
H	-3.475878	-3.947510	4.237215	H	-4.256801	-0.393366	5.008579
H	-7.250091	-2.962940	-0.610038	H	-5.648827	-3.962170	0.303924
H	-4.009496	-3.250679	-3.450372	H	-5.259091	-2.109394	-3.573425
H	1.189232	6.385907	2.661530	H	4.563497	4.724689	2.030591
H	-3.741261	4.229586	-4.933840	H	-0.897826	5.147670	-5.312101
H	-4.250385	-2.304416	5.943762	H	-5.585903	1.696531	5.281504
H	-6.349182	-3.792708	-2.780238	H	-6.019982	-4.016895	-2.159265
O	-3.815017	0.878603	0.419094	O	-3.708794	1.712273	-0.770316
N	-3.018571	1.974554	1.128686	N	-1.533451	3.541521	1.014663
				H	-2.499656	3.497798	0.675873

Table S7. Cartesian coordinates of the geometry optimized structure of **4a**$^{+}$ in the gas phase; PB86/def2-TZVP/ECP W, I).

I	0.404622	1.737228	-2.697860
W	-0.168652	0.782423	-0.123152
C	-1.266579	-1.271170	-3.196745
C	0.018911	4.631382	-0.386519

N	-2.043153	-0.076243	-1.091881
N	-1.468052	2.617828	0.094762
N	-1.155861	0.421601	1.815621
C	1.234083	1.987249	0.578733
C	0.597248	-1.150262	-0.046176
C	1.596144	-0.287418	0.233291
C	-2.292562	-0.764836	-2.239731
C	-1.262085	3.964702	-0.013052
N	-3.265721	0.185739	-0.523098
N	-2.786498	2.451186	0.459514
N	-2.528276	0.423503	1.891247
C	-0.693399	0.091016	3.051173
O	2.061705	2.703832	0.983323
P	0.404037	-2.910913	0.093310
P	3.425903	-0.553741	0.314671
C	-3.683233	-0.938710	-2.400343
C	-2.456654	4.649819	0.274280
C	-4.267882	-0.314660	-1.294545
B	-3.360278	1.047142	0.747696
C	-3.397908	3.658938	0.571520
C	-2.924619	0.102233	3.152403
C	0.748042	-0.015866	3.401242
C	-1.779160	-0.133856	3.919489
C	-1.093510	-3.349954	1.008060
C	0.389355	-3.721521	-1.529154
C	4.054057	-0.342147	2.012301
C	4.218784	0.656459	-0.771892
C	-4.362807	-1.620444	-3.548062
C	-2.649931	6.135194	0.251944
C	-5.716545	-0.158718	-0.960368
C	-4.835846	3.811127	0.947723
C	-4.360469	0.056962	3.563420
C	-1.697235	-0.521314	5.365049
C	-2.372822	-3.130081	0.466312
C	-0.963426	-3.964312	2.266387
C	1.500266	-3.495034	-2.366692
C	-0.599747	-4.643836	-1.908027
C	4.659324	-1.480293	2.575160
C	4.035386	0.861581	2.740728
C	5.203771	1.549958	-0.319403
C	3.919495	0.588402	-2.144975
C	-3.503127	-3.549985	1.168922
C	-2.101654	-4.379921	2.960819
C	1.599276	-4.172239	-3.581622
C	-0.487414	-5.318873	-3.127322
C	5.225350	-1.417925	3.850965

C	4.605180	0.915699	4.014623
C	5.872690	2.370218	-1.230665
C	4.591940	1.410291	-3.048686
C	-3.370484	-4.181043	2.410299
C	0.604690	-5.079929	-3.965587
C	5.197734	-0.221881	4.572925
C	5.567757	2.302296	-2.592853
H	-1.255584	-0.660780	-4.112103
H	0.639107	4.015364	-1.046868
H	-1.506843	-2.304214	-3.492248
H	-0.256829	-1.254016	-2.778088
H	-0.203472	5.571442	-0.910594
H	0.613621	4.888148	0.504148
H	-4.506337	1.138714	1.087628
H	0.870529	0.020805	4.491673
H	1.195074	-0.960681	3.052175
H	1.328909	0.803991	2.962928
H	-3.889009	-2.585649	-3.784475
H	-5.422013	-1.816643	-3.333134
H	-4.322449	-1.011084	-4.465287
H	-2.435349	6.557166	-0.742698
H	-3.681662	6.410605	0.507009
H	-1.987499	6.643264	0.969840
H	-6.321595	-0.803978	-1.610193
H	-5.932434	-0.423963	0.083611
H	-6.059362	0.876162	-1.114264
H	-5.117395	4.870919	0.920956
H	-5.499143	3.268817	0.258782
H	-5.036091	3.436117	1.962417
H	-4.446751	-0.357562	4.575617
H	-4.815628	1.058877	3.573907
H	-4.960246	-0.569509	2.888341
H	-1.180562	0.245258	5.964121
H	-2.696562	-0.651110	5.801201
H	-1.151992	-1.467289	5.506436
H	-2.491889	-2.629213	-0.495972
H	0.025021	-4.104081	2.704836
H	2.295289	-2.813220	-2.052108
H	-1.449521	-4.844916	-1.255053
H	4.704328	-2.403319	1.995877
H	3.585233	1.759424	2.318565
H	5.465289	1.595022	0.737661
H	3.165215	-0.110000	-2.509136
H	-4.492684	-3.387626	0.738778
H	-1.993498	-4.863007	3.933260
H	2.460848	-3.996700	-4.227853

H	-1.255134	-6.038012	-3.418027
H	5.698117	-2.305253	4.275719
H	4.590848	1.854969	4.570513
H	6.640555	3.058550	-0.873608
H	4.350682	1.355987	-4.111327
H	-4.258145	-4.515498	2.950367
H	0.687880	-5.609582	-4.916261
H	5.645424	-0.172442	5.567253
H	6.094353	2.943394	-3.302173
O	3.656377	-1.973883	-0.169210
N	1.686947	-3.451795	1.004796
H	1.754411	-4.470439	1.068950
H	2.579863	-3.027614	0.638823

4 References

[S1] G. M. Sheldrick, *SHELXS-2013, Program for Solution of Crystal Structure*, Univ. Göttingen, 2013.

[S2] G. M. Sheldrick, *SHELXL-2013, Program for Refinement of Crystal Structure*, Univ. Göttingen, 2013.

[S3] S. Parsons, B. Gould, R. Cooper and L. Farrugia, ROTAX 26th Version, Univ. Edinburgh, 2001.

[S4] A. L. Spek, *Acta Cryst*., 2009, **D65**, 148-155.

[S5] R. K. Harris and B. J. Kimber, *J. Magn. Reson.*, 1975, **17**, 174-188.

[S6] R. K. Harris, E. D. Becker, S. M. Cabral de Menezes, P. Granger, R. E. Hoffman and K. W. Zilm, *Pure Appl. Chem*., 2008, **80**, 59-84.

[S7] S. Trofimenko, *J. Am. Chem. Soc.*, 1967, **24**, 6288-6294.

[S8] N. G. Connelly and W. E. Geiger, *Chem. Rev.*, 1996, **96**, 877-910.

[S9] N. Burford, B. W. Royan, R. E. v. H. Spence, T. S. Cameron, A. Linden and R. D. Rogers, *J. Chem. Soc., Dalton Trans.*, 1990, 1521–1528.

[S10] M. Arisawa, T. Suzuki, T. Ishikawa and M. Yamaguchi, *J. Am. Chem. Soc.*, 2008, **130**, 12214–12215.

[S11] C. Bolli, J. Gellhaar, C. Jenne, M. Keßler, H. Scherer, H. Seeger and R. Uzun, *Dalton Trans*, 2014, **43**, 4326–4334.

[S12] G. Singh, *Phosphorus, Sulfur, and Silicon and the Related Elements*, 1994, **97**, 125–139.

[S13] C. B. Caputo, D. Winkelhaus, R. Dobrovetsky, L. J. Hounjet and D. W. Stephan, *Dalton Trans.*, 2015, **44**, 12256–12264.

[S14] F. Kunkel, H. Goesmann and K. Dehnicke, *Z. Naturforsch., B: J. Chem. Sci*, 1997, **52**, 1287–1290.

[S15] a) J. L. Holmes and F. P. Lossing, *J. Am. Chem. Soc.*, 1988, **110**, 7343–7345; b) Tschuikow-Roux and S. Paddison, *Int. J. Chem. Kinet.*, 1987, **19**, 15–24.

[S16] D. W. Ball, *Chem. Phys. Lett.*, 1999, **312**, 306–310.

[S17] D. R. Lide, ed., *CRC Handbook of Chemistry and Physics*, CRC Press, Boca Raton, 84th edn., 2003.

[S18] A. W. Shaw and A. J. Vosper, *J. Chem. Soc., Faraday Trans. 1*, 1977, **73**, 1239–1244.

[S19] a) S. Yasui, M. Tsujimoto, K. Shioji and A. Ohno, *Chem. Ber.*, 1997, **130**, 1699–1707; b) M. Nakamura, M. Miki and T. Majima, *J. Chem. Soc., Perkin Trans. 2*, 2000, 1447–1452; c) V. V. Yanilkin, *Russ. J. Electrochem.,* 2000, **36**, 219–226; d) S. Yasui, K. Itoh and A. Ohno, *Heteroatom Chem.*, 2001, **12**, 217–222.

[S20] *Gaussian 09*, Revision D.01, M. J. Frisch, G. W. Trucks, H. B. Schlegel, G. E. Scuseria, M. A. Robb, J. R. Cheeseman, G. Scalmani, V. Barone, B. Mennucci, G. A. Petersson, H. Nakatsuji, M. Caricato, X. Li, H. P. Hratchian, A. F. Izmaylov, J. Bloino, G. Zheng, J. L. Sonnenberg, M. Hada, M. Ehara, K. Toyota, R. Fukuda, J. Hasegawa, M. Ishida, T. Nakajima, Y. Honda, O. Kitao, H. Nakai, T. Vreven, J. A. Montgomery, Jr., J. E. Peralta, F. Ogliaro, M. Bearpark, J. J. Heyd, E. Brothers, K. N. Kudin, V. N. Staroverov, R. Kobayashi, J. Normand, K. Raghavachari, A. Rendell, J. C. Burant, S. S. Iyengar, J. Tomasi, M. Cossi, N. Rega, J. M. Millam, M. Klene, J. E. Knox, J. B. Cross, V. Bakken, C. Adamo, J. Jaramillo, R. Gomperts, R. E. Stratmann, O. Yazyev, A. J. Austin, R. Cammi, C. Pomelli, J. W. Ochterski, R. L. Martin, K. Morokuma, V. G. Zakrzewski, G. A. Voth, P. Salvador, J. J. Dannenberg, S. Dapprich, A. D. Daniels, Ö. Farkas, J. B. Foresman, J. V. Ortiz, J. Cioslowski and D. J. Fox, Gaussian, Inc., Wallingford CT, 2009.

[S21] a) F. Neese, *ORCA – An ab initio, DFT, and semi-empirical SCF-MO package*, 2012, version 3.0.2; b) F. Neese, The ORCA program system, *Wiley Interdiscip. Rev.: Comput. Mol. Sci.*, 2012, **2**, 73-78.

[S22] a) A. D. Becke, *J. Chem. Phys.*, 1986, **84**, 4524-4529; b) J. P. Perdew, *Phys. Rev. B*, 1986, **33**, 8522.

[S23] a) D. Andrae, U. Häußermann, M. Dolg, H. Stoll and H. Preuß, *Theor. Chim. Acta*, 1990, **77**, 123-141; b) J. M. L. Martin and A. Sundermann, *J. Chem. Phys.*, 2001, **114**, 3408-3420; c) A. Bergner, M. Dolg, W. Küchle, H. Stoll and H. Preuß, *Mol. Phys.*, 1993, **80**, 1431-1441.

[S24] F. Weigend and R. Ahlrichs, *Phys. Chem. Chem. Phys.*, 2005, **7,** 3297-3305.

[S25] a) J. P. Perdew, K. Burke and M. Ernzerhof, *Phys. Rev. Lett.*, 1996, **77**, 3865-3868; b) J. P. Perdew, K. Burke and M. Ernzerhof, *Phys. Rev. Lett.*, 1997, **78**, 1396; c) C. Adamo and V. Barone, *J. Chem. Phys.*, 1999, **110**, 6158-6169.

[S26] a) D. A. Pantazis, X. Y. Chen, C. R. Landis and F. Neese, *J. Chem. Theory Comput.*, 2008, **4**, 908; b) D. A. Pantazis and F. Neese, *J. Chem. Theory Comput.*, 2009, **5**, 2229.

[S27] a) S. Grimme, S. Ehrlich and L. Goerigk, *J. Comput. Chem.*, 2011, **32**, 1456-1465; b) S. Grimme, J. Antony, S. Ehrlich and H. Krieg, *J. Chem. Phys.*, 2010, **132**, 154104.